

Supporting Information

Specific stereoisomeric conformations determine the drug potency of cladospirin scaffold against malarial parasite

Pronay Das^{†ab}, Palak Babbar^{†c}, Nipun Malhotra^{†c}, Manmohan Sharma^c, Goraknath R. Jachak^{ab}, Rajesh G. Gonnade^{bd}, Dhanasekaran Shanmugam^{be}, Karl Harlos^f, Manickam Yogavel^c, Amit Sharma^{c*}, and D. Srinivasa Reddy^{ab*}

^aCSIR-National Chemical Laboratory, Dr. Homi Bhabha Road, Pune 411008, India

^bAcademy of Scientific and Innovative Research (AcSIR), New Delhi 110025, India

^cMolecular Medicine Group, International Centre for Genetic Engineering and Biotechnology (ICGEB), New Delhi 110067, India

^dCenter for Material Characterization, CSIR-National Chemical Laboratory, Dr. Homi Bhabha Road, Pune 411008, India

^eBiochemical Sciences Division, CSIR-National Chemical Laboratory, Dr. Homi Bhabha Road, Pune 411008, India

^fDivision of Structural Biology, Wellcome Trust Centre for Human Genetics, The Nuffield Department of Medicine, University of Oxford, Oxford OX3 7BN, UK

[†]All three have contributed equally to this work.

Table of Content

1) Single Crystal X-ray and ORTEP.....	S3 – S6
2) Protein Expression and Purifications.....	S6
3) Thermal Shift Assay.....	S6
4) Aminoacylation Assay.....	S7
5) <i>P. falciparum</i> culture.....	S8
6) Crystallization.....	S9 – S10
7) ¹ H and ¹³ C NMR Spectra.....	S11 – S37
8) References.....	S38

Single crystal X- ray diffraction:

X-ray intensity data measurements of compounds compound **16**, compound **17**, compound **18** and compound **19** were carried out on a Bruker D8 VENTURE Kappa Duo PHOTON II CPAD diffractometer equipped with Incoatech multilayer mirrors optics. The intensity measurements were carried out at 100(2) K temperature with Mo micro-focus sealed tube diffraction source ($\text{MoK}_\alpha = 0.71073 \text{ \AA}$) on compounds **17**, **18** and **19** whereas for compound **16** the Cu micro-focus sealed tube diffraction source ($\text{CuK}_\alpha = 1.54178 \text{ \AA}$) was used. The X-ray generator was operated at 50 kV and 1.1 mA (for Cu source) and 50 kV and 1.4 mA (for Mo source). A preliminary set of cell constants and an orientation matrix were calculated from three sets of 36 frames for compounds compound **17**, compound **18** and compound **19** whereas two sets of 40 frames for compound compound **16**. Data were collected with ω scan width of 0.5° at different settings of φ and 2θ with a frame time of 10-20 secs (depending on the diffraction power of the crystal) keeping the sample-to-detector distance fixed at 5.00 cm. The X-ray data collection was monitored by APEX3 program¹. All the data were corrected for Lorentzian, polarization and absorption effects using SAINT and SADABS programs¹. SHELX-97 was used for structure solution and full matrix least-squares refinement on F^2 ². All the hydrogen atoms were placed in a geometrically idealized positions and constrained to ride on its parent atoms. An ORTEP III³ view of compounds was drawn with 50% probability displacement ellipsoids and H atoms are shown as small spheres of arbitrary radii.

Crystal data of compound 16: $\text{C}_{16}\text{H}_{20}\text{O}_5$, $M = 292.32$, colorless needle, $0.24 \times 0.08 \times 0.05 \text{ mm}^3$, orthorhombic, chiral space group $P2_12_12_1$, $a = 7.5165(16) \text{ \AA}$, $b = 8.0959(17) \text{ \AA}$, $c = 24.661(9) \text{ \AA}$, $V = 1500.7(7) \text{ \AA}^3$, $Z = 4$, $T = 100(2) \text{ K}$, $2\theta_{\text{max}} = 144^\circ$, $D_{\text{calc}} (\text{g cm}^{-3}) = 1.294$, $F(000) = 624$, $\mu (\text{mm}^{-1}) = 0.792$, 25100 reflections collected, 2929 unique reflections ($R_{\text{int}} = 0.0342$, $R_{\text{sig}} = 0.0215$), 2901 observed ($I > 2\sigma(I)$) reflections, multi-

scan absorption correction, $T_{\min} = 0.833$, $T_{\max} = 0.961$, 193 refined parameters, Good of Fit = $S = 1.110$, $R1 = 0.0307$, $wR2 = 0.0788$ (all data $R = 0.0310$, $wR2 = 0.0785$), maximum and minimum residual electron densities; $\Delta\rho_{\max} = 0.230$, $\Delta\rho_{\min} = -0.160$ ($\text{e } \text{\AA}^{-3}$). The absolute configuration for compound **16** was established by the structure determination of a compound containing a chiral reference molecule of known absolute configuration and confirmed by anomalous dispersion effects in diffraction measurements on the crystal (Flack parameter, 0.05(4)). The single crystal X-ray diffraction data analysis clearly established that our synthesized compound has *R*, *R*, and *R*, configurations at C8, C11, and C15 positions respectively for compound **16**.

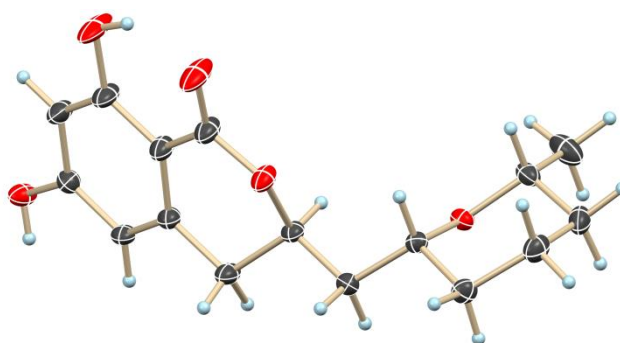


Figure 1: ORTEP diagram of compound **16**

Crystal data of compound 17: $\text{C}_{16}\text{H}_{20}\text{O}_5$, $M = 292.32$, colorless needle, $0.27 \times 0.09 \times 0.07 \text{ mm}^3$, monoclinic, chiral space group $P2_1$, $a = 7.7904(6) \text{ \AA}$, $b = 11.4929(11) \text{ \AA}$, $c = 16.2869(15) \text{ \AA}$, $\beta = 103.739(3)$, $V = 1416.5(2) \text{ \AA}^3$, $Z = 4$, $T = 100(2) \text{ K}$, $2\theta_{\max} = 50^\circ$, D_{calc} (g cm^{-3}) = 1.371, $F(000) = 624$, μ (mm^{-1}) = 0.101, 14984 reflections collected, 4894 unique reflections ($R_{\text{int}} = 0.0519$, $R_{\text{sig}} = 0.0549$), 4416 observed ($I > 2\sigma(I)$) reflections, multi-scan absorption correction, $T_{\min} = 0.973$, $T_{\max} = 0.993$, 386 refined parameters, Good of Fit = $S = 1.049$, $R1 = 0.0389$, $wR2 = 0.0784$ (all data $R = 0.0457$, $wR2 = 0.0808$), maximum and minimum residual electron densities; $\Delta\rho_{\max} = 0.235$, $\Delta\rho_{\min} = -0.178$ ($\text{e } \text{\AA}^{-3}$).

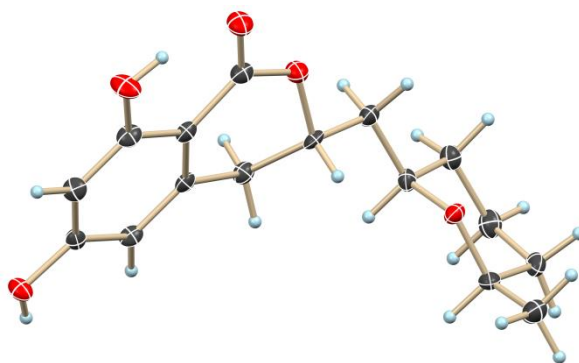


Figure 2: ORTEP diagram of compound **17**

Crystal data of compound 18: $C_{16}H_{20}O_5$, $M = 292.32$, colorless needle, $0.15 \times 0.07 \times 0.03 \text{ mm}^3$, orthorhombic, chiral space group $P2_12_12_1$, $a = 6.9288(8) \text{ \AA}$, $b = 7.9172(9) \text{ \AA}$, $c = 52.844(6) \text{ \AA}$, $V = 2898.9(6) \text{ \AA}^3$, $Z = 4$, $T = 100(2) \text{ K}$, $2\theta_{\text{max}} = 52.8^\circ$, $D_{\text{calc}} (\text{g cm}^{-3}) = 1.340$, $F(000) = 1248$, $\mu (\text{mm}^{-1}) = 0.099$, 39126 reflections collected, 5904 unique reflections ($R_{\text{int}} = 0.1157$, $R_{\text{sig}} = 0.1067$), 4006 observed ($I > 2\sigma(I)$) reflections, multi-scan absorption correction, $T_{\text{min}} = 0.985$, $T_{\text{max}} = 0.997$, 431 refined parameters, no of restraints = 108, Good of Fit = $S = 1.163$, $R1 = 0.1018$, $wR2 = 0.1704$ (all data $R = 0.1524$, $wR2 = 0.1864$), maximum and minimum residual electron densities; $\Delta\rho_{\text{max}} = 0.331$, $\Delta\rho_{\text{min}} = -0.342 (\text{e \AA}^{-3})$.

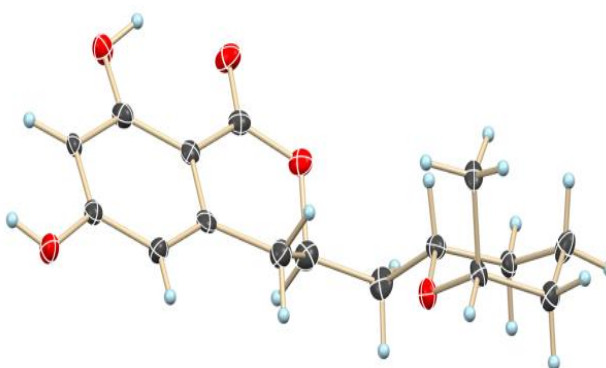


Figure 3: ORTEP diagram of compound **18**

Crystal data of compound 19: $C_{16}H_{20}O_5$, $M = 292.32$, colorless plate, $0.33 \times 0.11 \times 0.05 \text{ mm}^3$, tetragonal, chiral space group $P4_32_12$, $a = 8.0784(3) \text{ \AA}$, $c = 45.237(2) \text{ \AA}$, $V = 2952.2(3) \text{ \AA}^3$, $Z = 8$, $T = 100(2) \text{ K}$, $2\theta_{\text{max}} = 56^\circ$, $D_{\text{calc}} (\text{g cm}^{-3}) = 1.315$, $F(000) = 1248$, μ

(mm⁻¹) = 0.097, 58733 reflections collected, 3539 unique reflections ($R_{\text{int}} = 0.0234$, $R_{\text{sig}} = 0.0087$), 3519 observed ($I > 2\sigma(I)$) reflections, multi-scan absorption correction, $T_{\text{min}} = 0.969$, $T_{\text{max}} = 0.995$, 193 refined parameters, Good of Fit = $S = 1.084$, $R1 = 0.0301$, $wR2 = 0.0803$ (all data $R = 0.0303$, $wR2 = 0.0805$), maximum and minimum residual electron densities; $\Delta\rho_{\text{max}} = 0.289$, $\Delta\rho_{\text{min}} = -0.136$ (e Å⁻³). The absolute configuration was established by the structure determination of a compound containing a chiral reference molecule of known absolute configuration and confirmed by anomalous dispersion effects in diffraction measurements on the crystal (Flack parameter, 0.09(10)). The single crystal X-ray diffraction data analysis clearly established that our synthesized compound has *S*, *S*, and *R*, configurations at C8, C11, and C15 positions respectively for compound **19**.

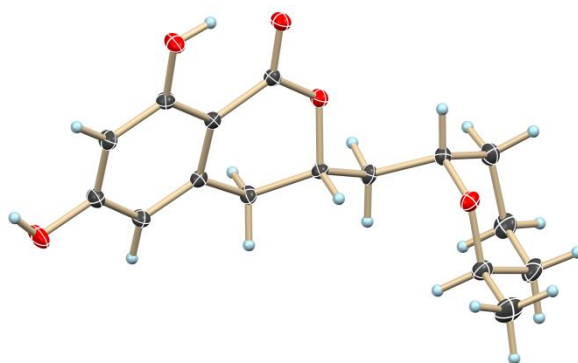


Figure 4: ORTEP diagram of compound **19**

Protein expressions and purifications:

Pf-KRS and *Hs*-KRS were produced in *E. coli* BL-21 strain in accordance with the methods already published. Highly pure enzymes, post-gel filtration chromatography, were stored in 50mM Tris-HCl pH 8.0, 200mM NaCl, 10mM βME at -80 °C.

Thermal shift assays:

These were performed for both *Pf*-KRS and *Hs*-KRS in presence of eight cladologs as per methods described earlier^{4,5}. Briefly, purified proteins alone and/or with different cladologs were heated from 25 to 99 °C at a rate of 1 °C min⁻¹ and fluorescence signals of the

SYPRO® orange dye were monitored by StepOnePlus™ quantitative real-time PCR system (Life Technologies). Data were analysed on Protein Thermal shift software (ThermoFisher). Mean value from triplicates are presented as points. No protein controls along with buffers with only inhibitors were used as blanks and flat lines were observed for these fluorescence readings across the temperatures.

Aminoacylation assays:

For this complementary DNA oligonucleotides were purchased from Sigma with one primer containing the T7 RNA polymerase promoter followed by gene encoding the tRNA^{lys} while the other primer encoded the complementary strand with promoter and the tRNA gene. These two oligos were mixed in equimolar ratios in an annealing buffer (10 mM Tris pH 8.0, 50 mM NaCl and 0.5 mM EDTA), heated to 95 °C and then slow cooled at room temperature. Using Ambion Maxiscript T7 *in-vitro* transcription kit *in vitro* transcription reaction was done, using this annealed dsDNA to produce tRNA^{lys}. The enzymatic assays were done according to an earlier report⁶. The standard aminoacylation reaction ingredients were aminoacylation buffer 30 mM HEPES buffer pH 7.4, 140 mM NaCl, 30 mM KCl, 40 mM MgCl₂, 1 mM DTT, 100 μM ATP, 500 μM L-lys (Sigma-Aldrich), 10 μM tRNA^{lys}. For KRS inhibition, a reaction solution containing individual KRS (0.4 μM for *Pf*-KRS and 0.2 μM for *Hs*-KRS) was mixed with cladologs at 1 nM to 100 μM in 100 μl volume and incubated at 37 °C for ~45 min and 1 h respectively. Assays were done with the help of AMP-GLO kit (www.promega.in/products/cell-signaling/signaling-pathway-assays/amp_glo-assay) and a non-linear regression curve i.e the percent enzyme activity versus different inhibitor concentration (log₁₀ scale) were plotted using Prism (GraphPad). All data are shown as means ± SD, from at least two independent assays performed in triplicate.

P. falciparum culture:

The strain 3D7 was cultured in O⁺ erythrocytes in RPMI 1640 (Invitrogen, USA) supplemented with 4.5 mg mL⁻¹ glucose (Sigma, USA), 0.1 mM hypoxanthine (Invitrogen, USA), 25 mg mL⁻¹ gentamicin (Invitrogen, USA) and 0.5% AlbuMax-I (Invitrogen, USA), according to standard methods⁷. Synchronised culture was maintained by treating ring stage parasite with sorbitol as described⁸. For inhibition assays, 20mM stocks were prepared for Cladologs in DMSO (Sigma). *Plasmodium falciparum* was cultured in 96-well plates and synchronized at ring stages. At ~1% parasitemia and 4% hematocrit, inhibitor concentration ranges from 15 nM to 4 μ M were incubated for 48 hours with the parasites. Growth was assayed by SYBR green-I (Molecular probes) DNA staining assays as described earlier⁹. Briefly, 100 μ l SYBR green dye in 1 \times concentration in lysis buffer supplemented with 0.1% saponin was added to each well. After 45 min incubation at 37 °C fluorescence was estimated using multi-well plate reader (Victor 3, Perkin Elmer) with excitation and emission wavelength bands centered at 485 and 530 nm respectively. Chloroquine was taken as a positive control and all experiments were done in triplicates. The EC₅₀ values were obtained by plotting a nonlinear regression curve as a function of fluorescence values expressed in terms of percentage inhibition of parasite growth at each inhibitor concentration using GraphPad Prism. All data are shown for three replicates as means with standard errors.

Crystallization:

Highly pure Pf-KRS was stored at 15mg/mL -80°C. Before crystallization, 0.5 mM inhibitors along with 2 mM l-lysine were added to 13 mg mL⁻¹ protein solutions and incubated at 4° C for 30 min. The Pf-KRS/cladolog crystals were obtained using hanging-drop vapour-diffusion method at 20° C. Initial screenings were carried out using nano-drop dispensing robot Mosquito (TTP Labtech) and the droplet size was a mixture of 100 nano-litres of Pf-

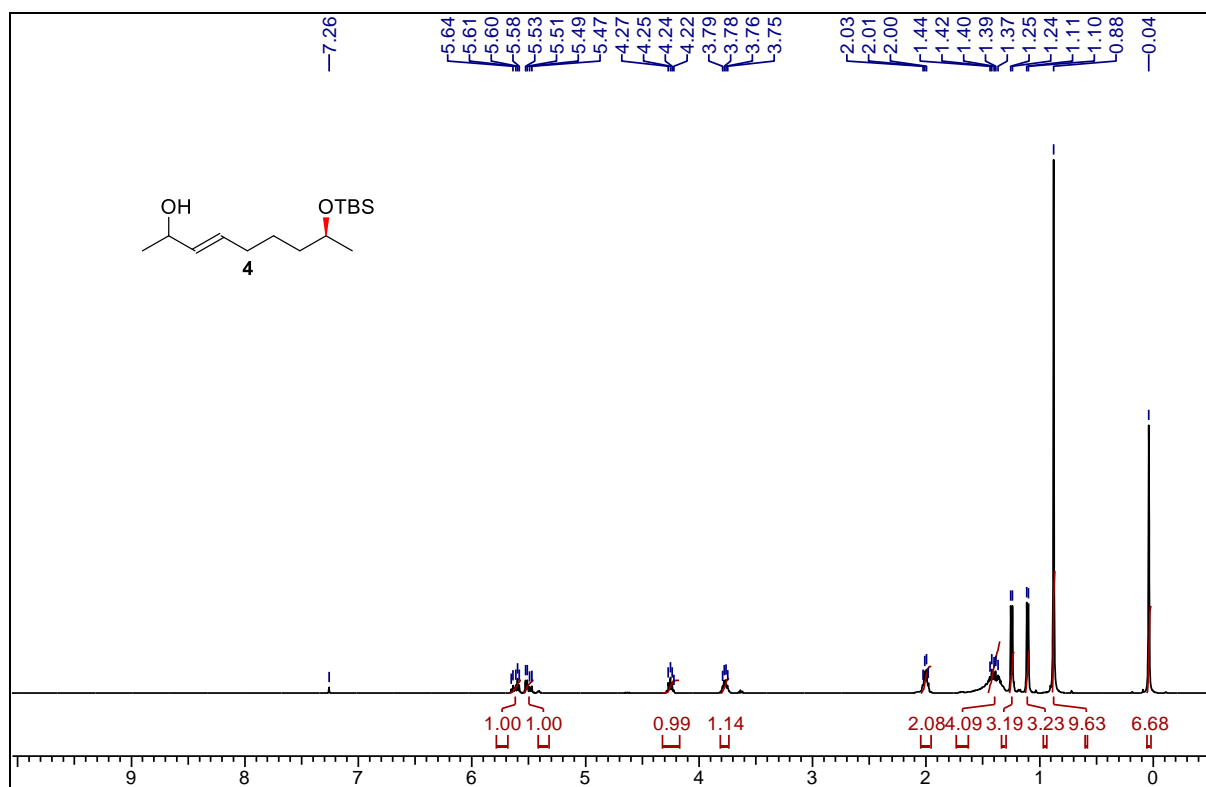
KRS+L-Lys+cladologs complex and 100 nl of well solutions from commercial crystal screens (Hampton Research and Molecular Dimensions). The crystallization drops were equilibrated against 75/100 mL well reservoir solutions using commercially available Morpheous screening reagents from Molecular Dimensions Ltd.

Data collection and structure determination of KRS-cladolog complexes:

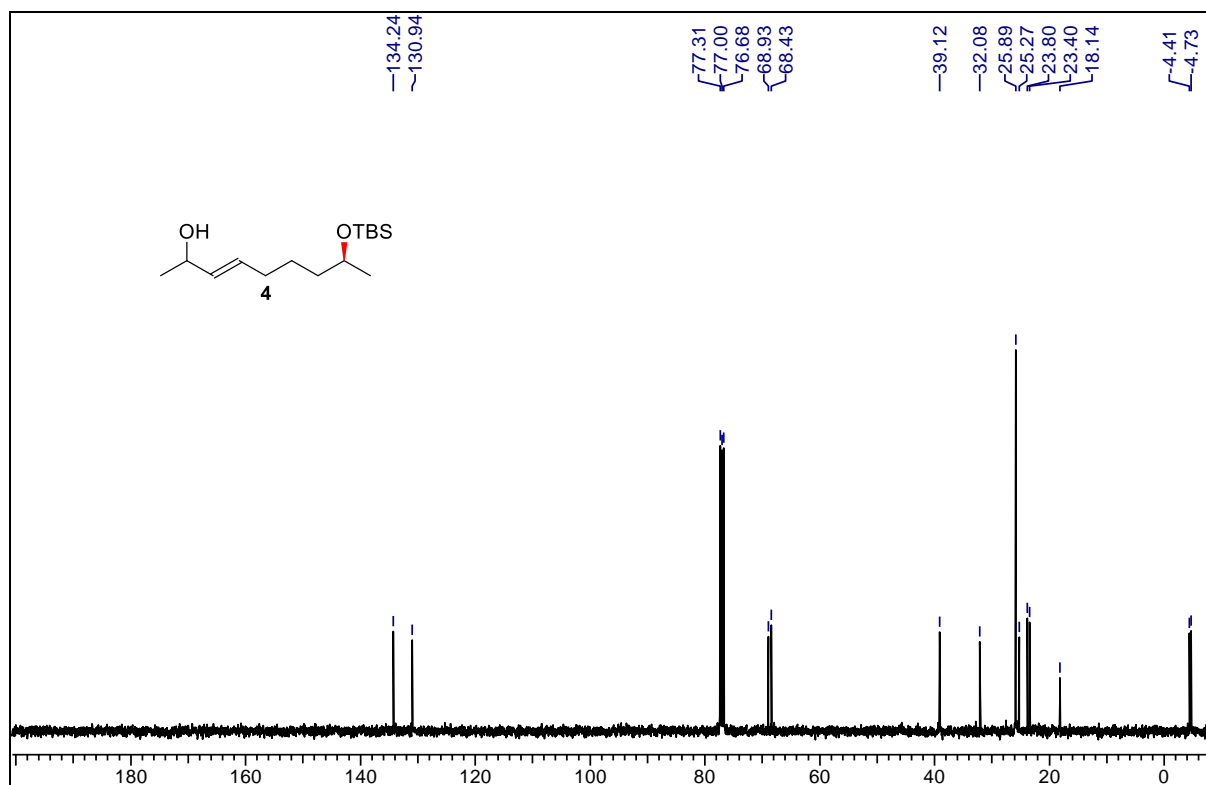
X-ray diffraction data were collected using multiple beam-lines at Diamond Light Source (DLS) and Synchrotron SOLEIL at 100 K with 0.1° increments per image, for a total of 3600 images. The data were auto-processed using X-ray Detector Software (XDS)/XSCALE¹⁰, diffraction integration for advanced light sources¹¹. The structures were solved by molecular replacement in PHASER using *Pf*KRS-apo structure (PDB code: 4TWA) as the template. All models were initially refined using REFMAC5¹² and completed with *phenix.refine* in PHENIX¹³. Cladologs and water molecules were added into the electron density maps using COOT¹⁴. X-ray refinement restraint parameters were generated for cladologs using COOT34 and Sketcher program in CCP4 Suite¹⁵. The quality of the final models and bound ligands was verified using composite simulated annealing omit (SA-omit) maps. The occupancies of bound ligands and alternate conformations of protein residues were refined and confirmed using omit maps. The final model quality was analyzed using MolProbity¹⁶. Statistics for data collection and structure refinements are given in Table 3. All structural superposition and preparation of figures was done using UCSF Chimera¹⁷ and PyMOL (<http://www.pymol.org>). The atomic coordinates and structure factors for the four structures have been deposited into Protein Data Bank with accession codes 5ZH5 for compound **13**; 5ZH2 for compound **16**; 5ZH3 for compound **17** and 5ZH4 for compound **18**.

	Compound 18	Compound 16	Compound 13	Compound 17
Source	I03, DLS	I03, DLS	I03, DLS	I03, DLS
Wavelength (Å)	0.09763	0.09763	0.09763	0.09763
Oscillation width (°)	0.1	0.1	0.1	0.1
Exposure time (s)	0.02	0.02	0.02	0.02
Transmission %	100	100	100	100
Flux	1.05e ⁺¹²	6.24e ⁺¹¹	6.31e ⁺¹¹	6.30e ⁺¹¹
Beam size (µm)	80 x 20	50 x 20	50 x 20	50 x 20
Cell parameters (Å, °)	52.62, 126.04, 181.19; 90.0, 90.0, 90.00	52.81, 126.15, 181.57; 90.0, 90.0, 90.0	54.50, 130.36, 174.69; 90.0, 90.0, 90.0	54.30, 130.40, 174.21; 90.0, 90.0, 90.00
Space group	P2 ₁ 2 ₁ 2 ₁	P 2 ₁ 2 ₁ 2 ₁	P 2 ₁ 2 ₁ 2 ₁	P 2 ₁ 2 ₁ 2 ₁
Resolution	40.93-2.60 (2.64-2.60)	47.05-2.66 (2.71-2.66)	42.17 – 3.08 (3.13-3.08)	52.20-2.82 (2.87-2.82)
Observations	497691	461588	304079	388856
No. of observed unique reflections	38068	35718 (1744)	23820 (1153)	30082 (1449)
I/σ (I)	11.8 (1.3)	8.5 (1.4)	9.2 (1.2)	12.8 (1.5)
R _{meas}	0.164 (2.425)	0.277 (2.024)	0.321 (2.517)	0.133 (1.672)
Completeness	100 (100)	99.8 (100)	100 (99.8)	98.8 (99.9)
Redundancy	13.1 (13.0)	12.9 (13.8)	12.8 (12.9)	12.9 (13.6)
Molecules/ASU	2			
% Solvent/ V _m (Å ³ /Da)				
Refinement Resolution (Å)	40.93-2.60 (2.66-2.60)	47.05-2.66 (2.73-2.66)	42.17 – 3.08 (3.16-3.08)	52.20-2.82 (2.89-2.82)
R _{factor} /R _{free}	21.2 (27.2)/26.9 (34.7)	20.8 (28.6)/26.6 (38.3)	23.2 (37.7) / 27.8 (33.2)	25.2 (43.0)/28.7 (37.4)
Reflections used in refinement (>σ)	36090	33866	22625	28554
Reflections in working set	34278(2619)	32069 (2459)	21484 (1625)	27090 (2033)
Test set	1912 (132)	1797 (126)	1141 (81)	1464 (119)
Number of atoms				
Total				
Protein	7299	7640	7846	7846
Ligands (Lys/CLD/others)	20/42/17	20/42/3	20/42	20/42
Water				
B-factors (Å ²)				
Protein	53.7	38.0	102.7	65.3
Ligands	44.6	24.9	87.3	31.3
Ramachandran plot (outlier/favoured/allowed/total)	9/889/924/933	10/906/950/960	3/934/963/966	8/1863/1924/1932
R.m.s deviation				
Bond lengths (Å)	0.011	0.009	0.009	0.010
Bond angles (°)	1.576	1.456	1.376	1.503

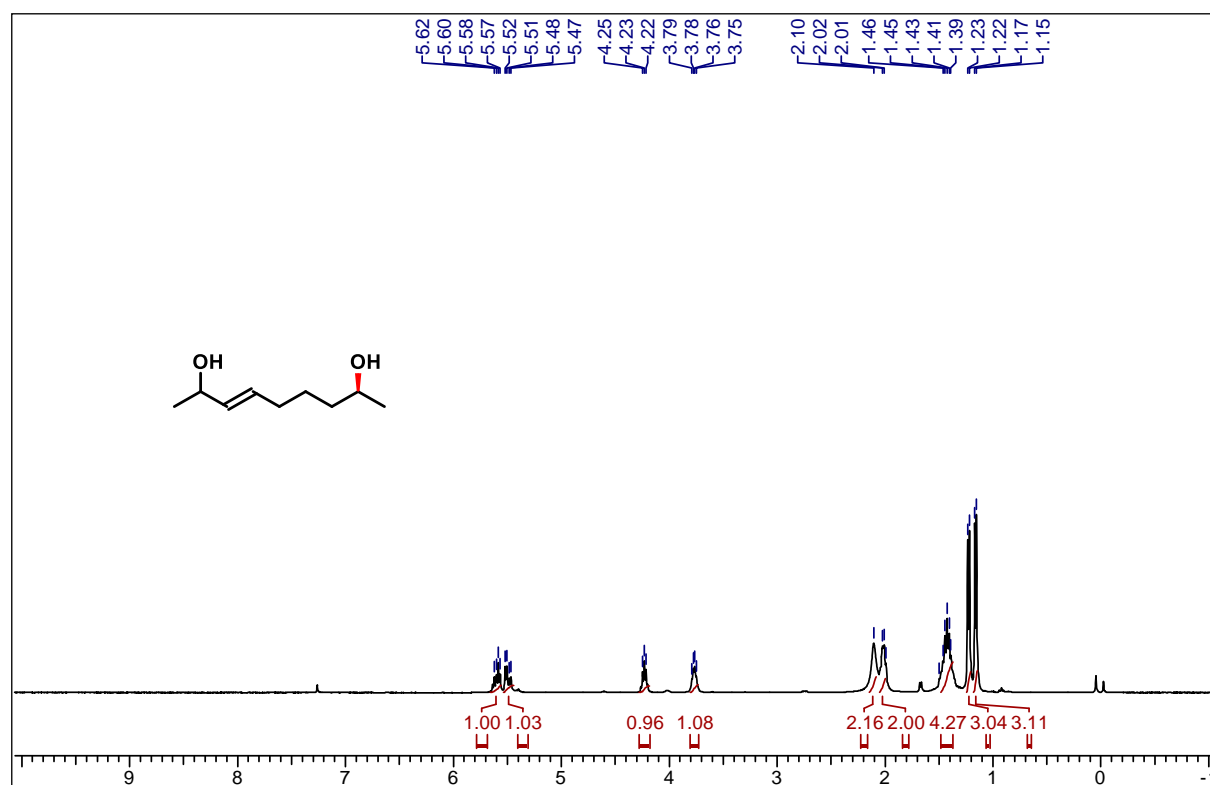
^1H NMR spectra of compound 4 in 400 MHz



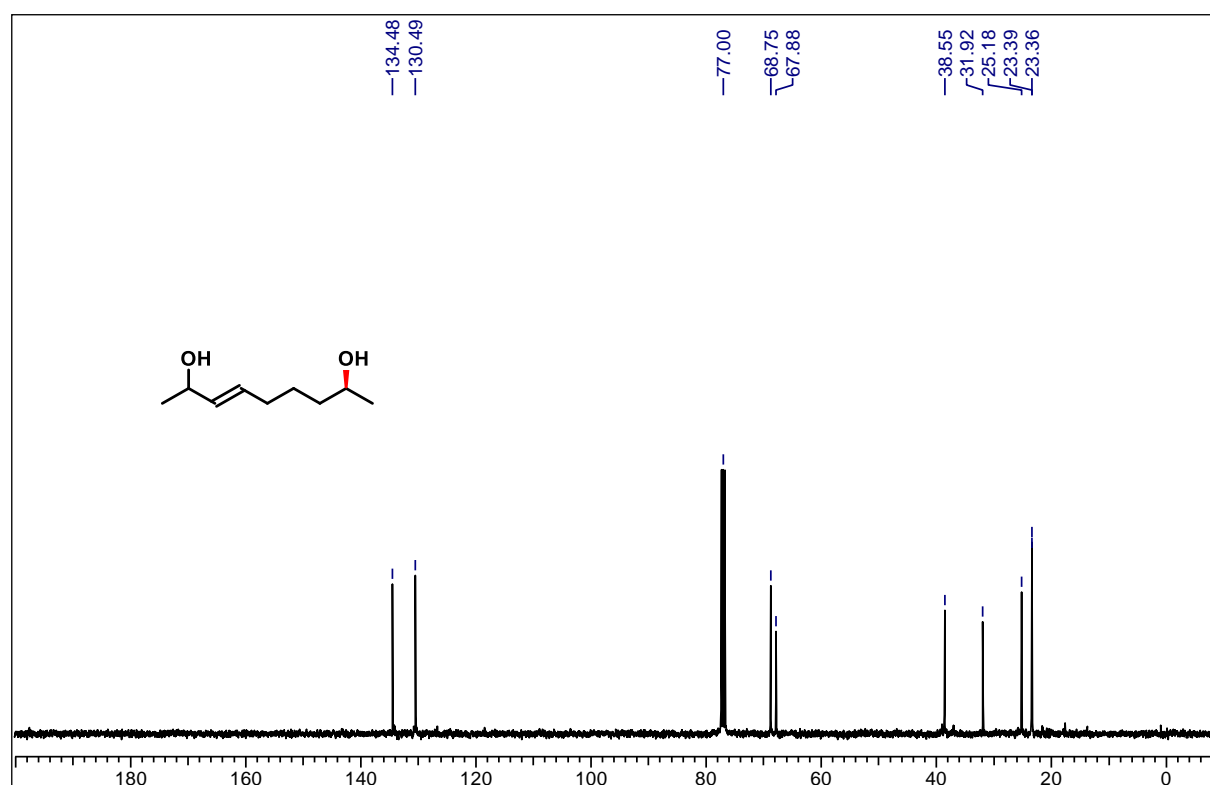
^{13}C NMR spectra of compound 4 in 100 MHz



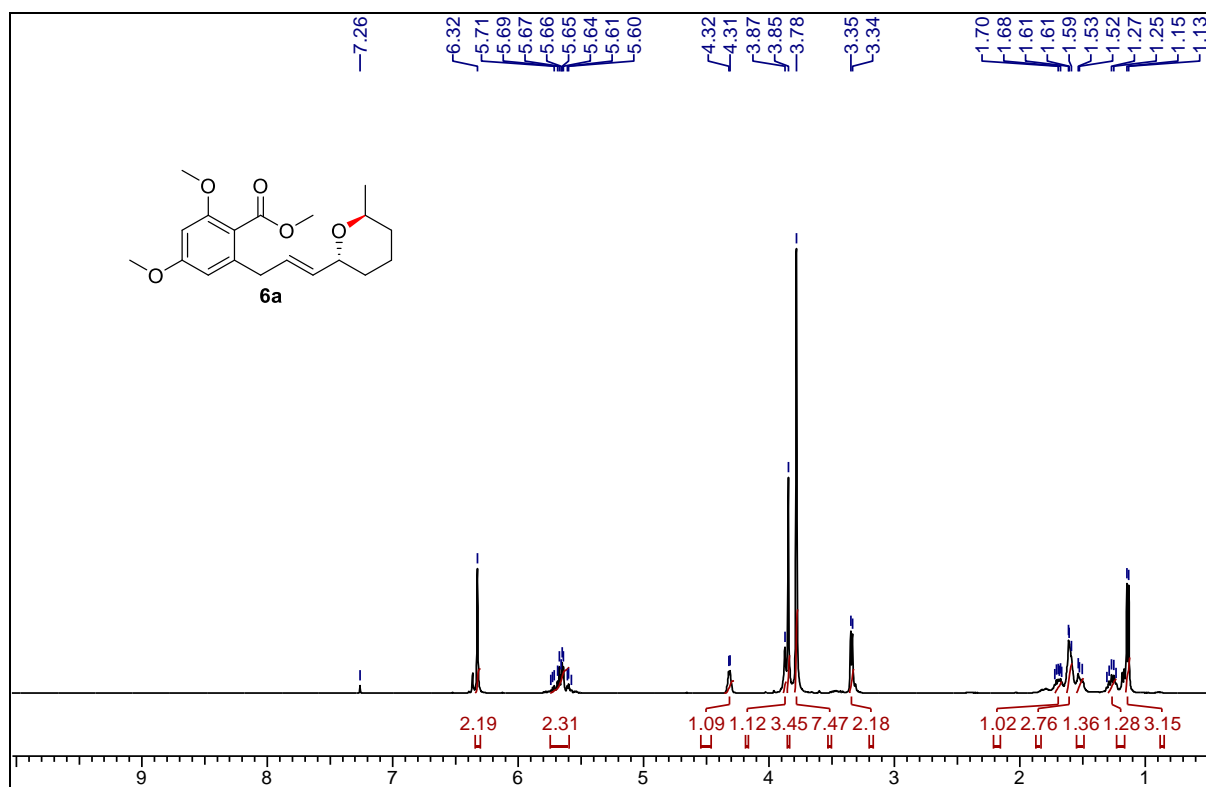
^1H NMR spectra of compound 5 in 400 MHz



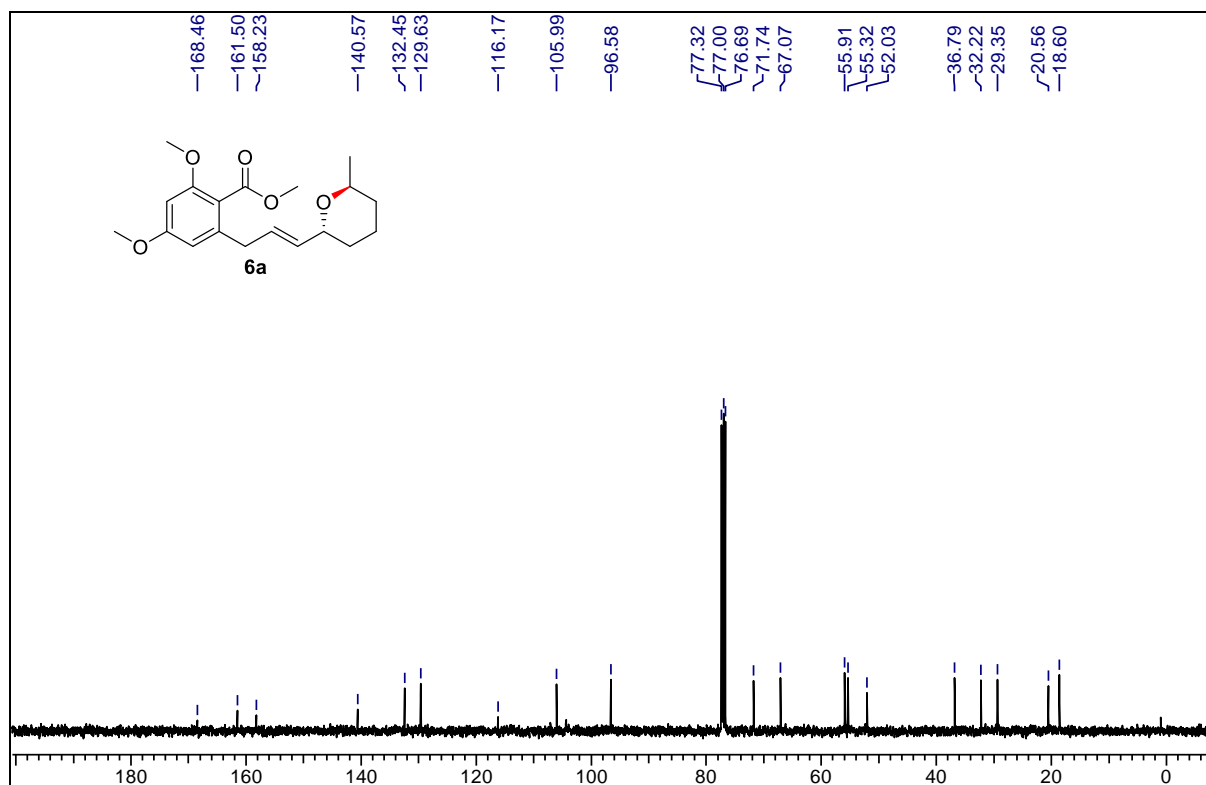
^{13}C NMR spectra of compound 5 in 100 MHz



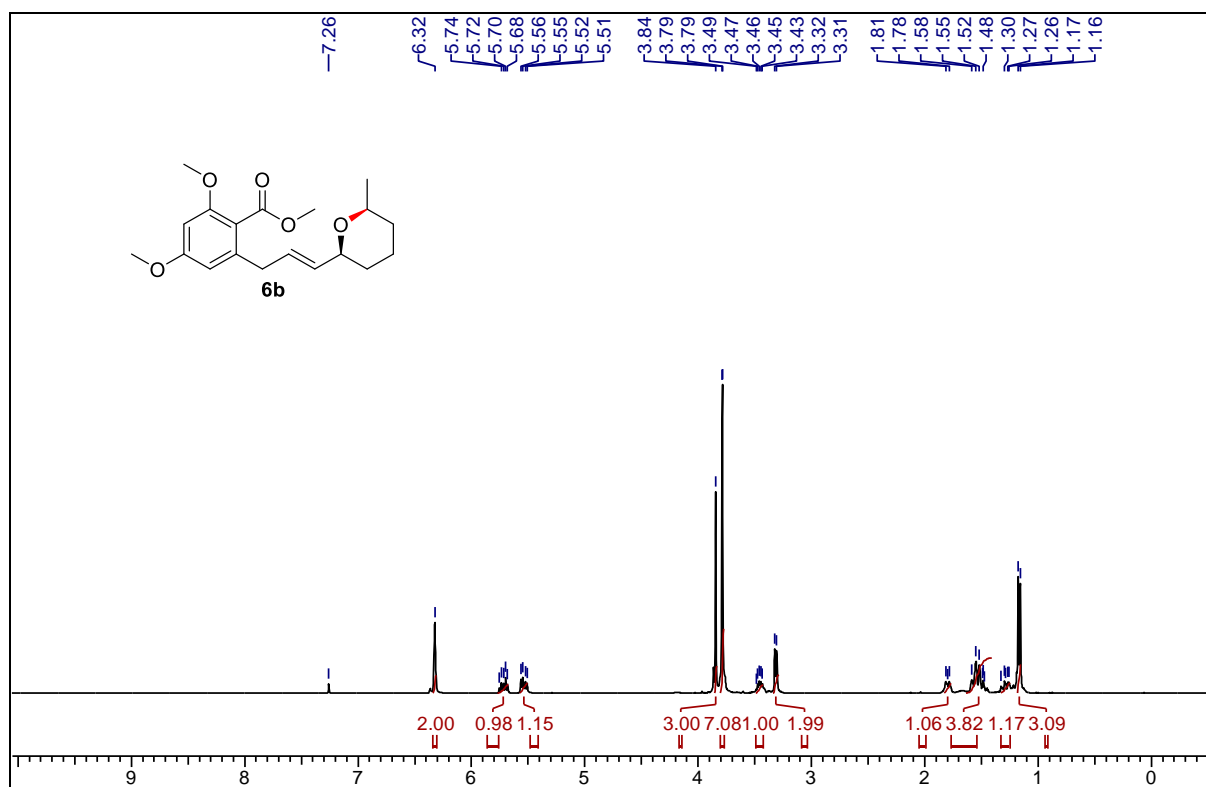
¹H NMR spectra of compound 6a in 400 MHz



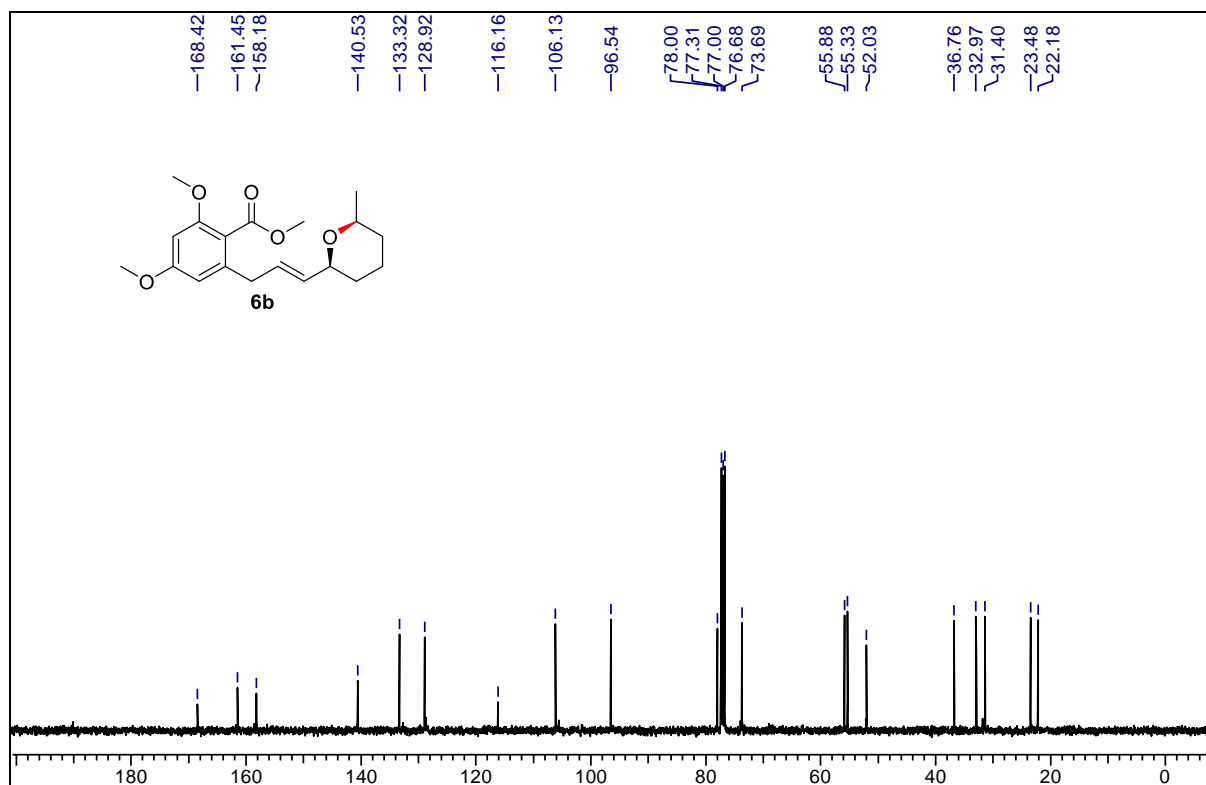
¹³C NMR spectra of compound 6a in 100 MHz



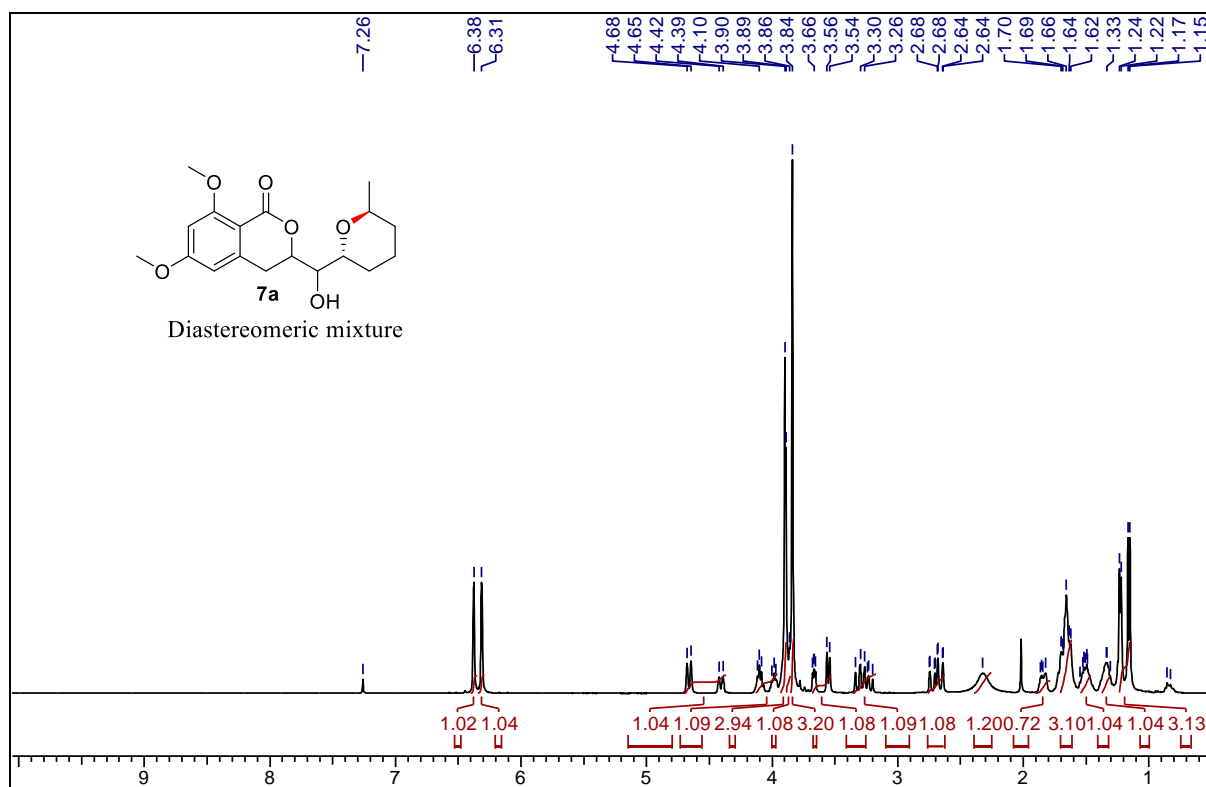
¹H NMR spectra of compound 6b in 400 MHz



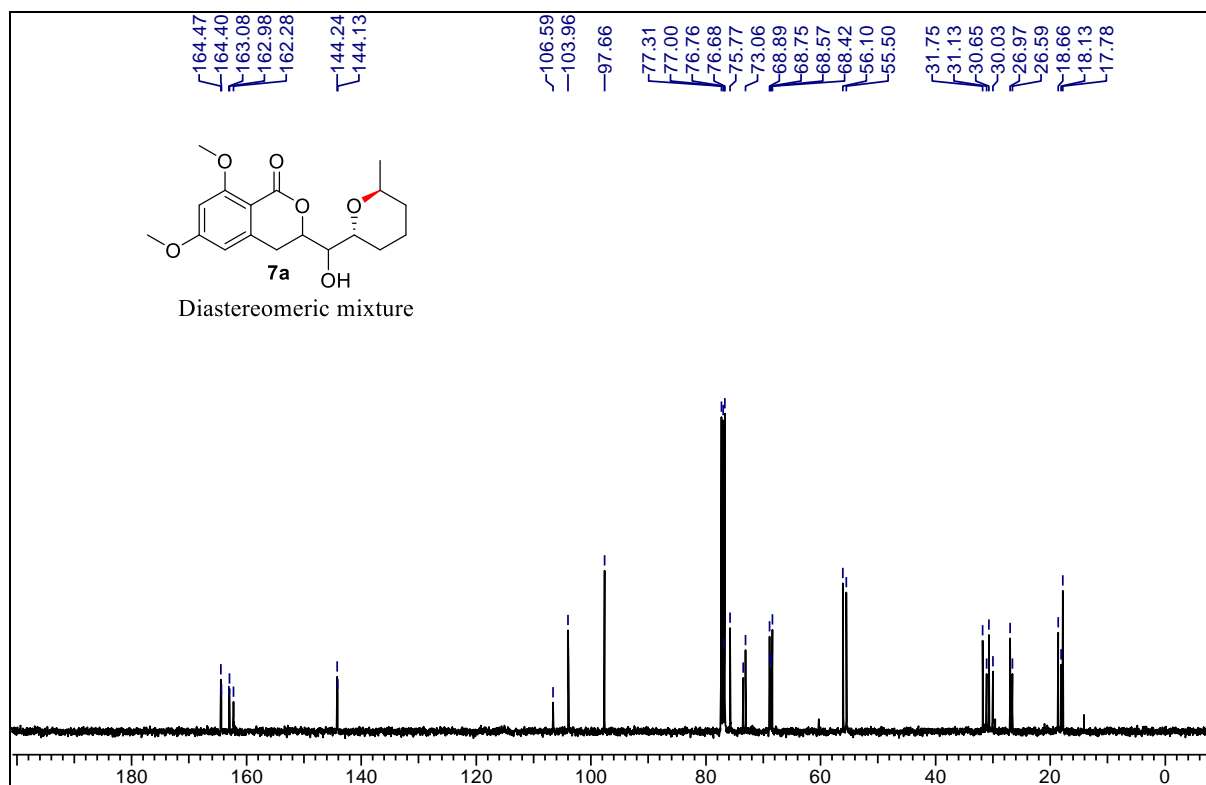
¹³C NMR spectre of compound 6b in 100 MHz



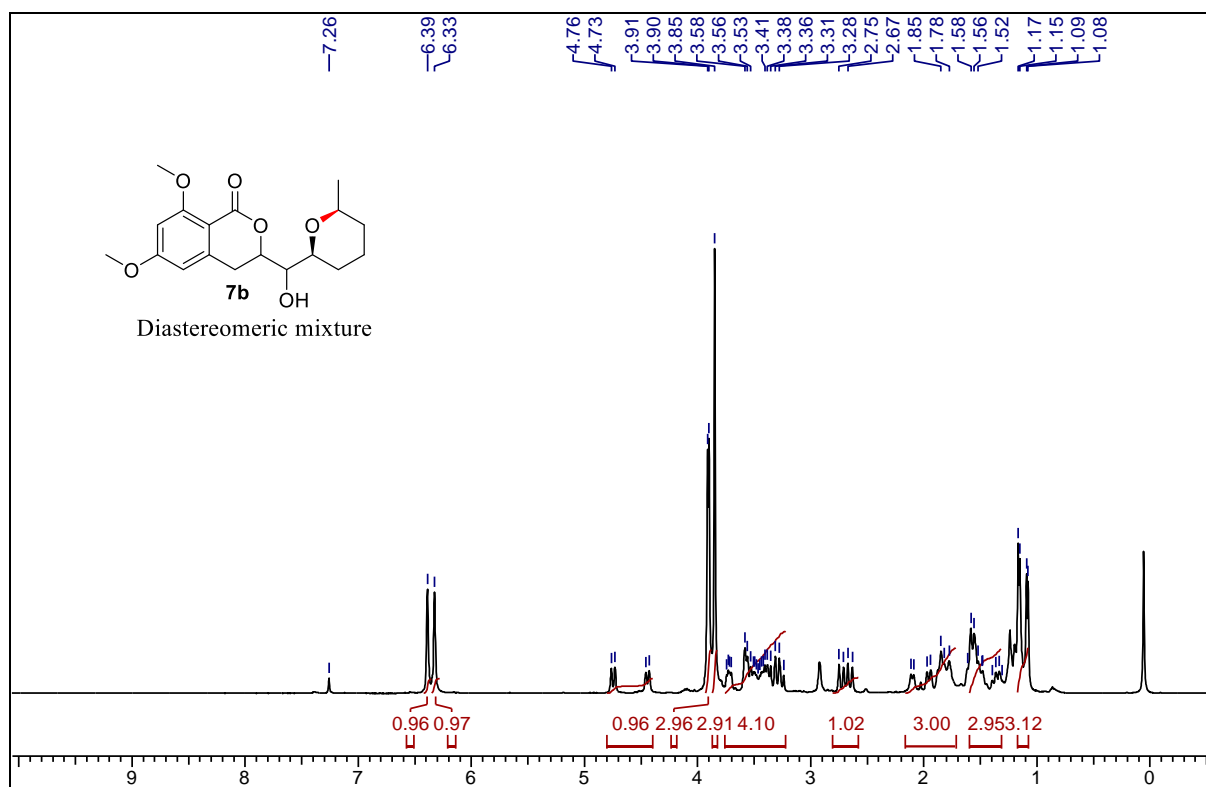
¹H NMR spectra compound 7a in 400 MHz



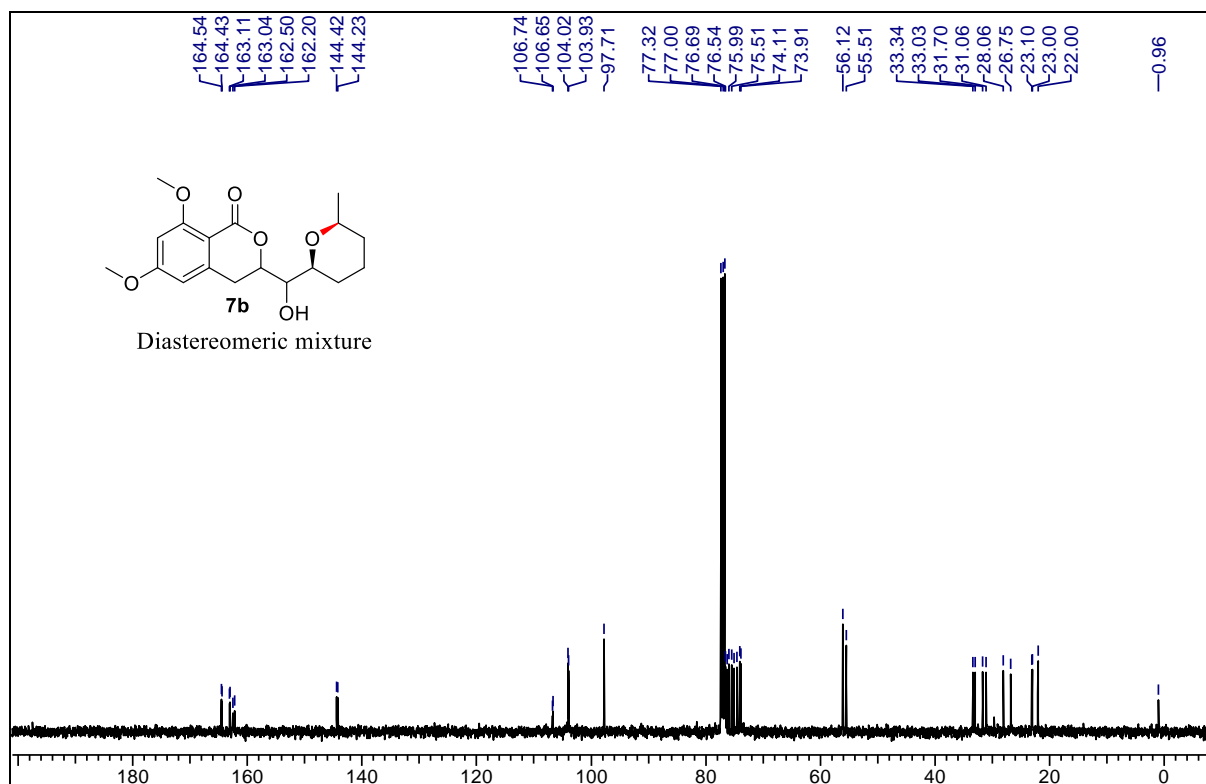
¹³C NMR spectra compound 7a in 100 MHz



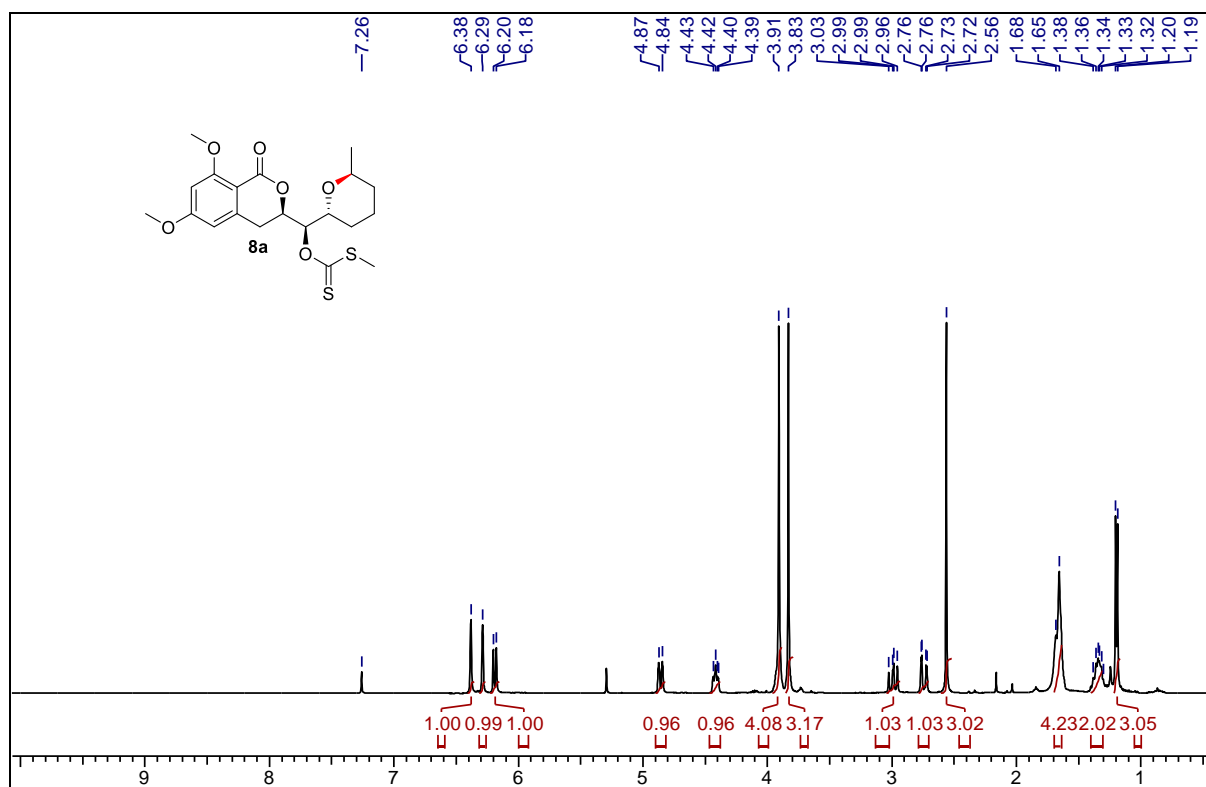
¹H NMR spectra of compound 7b in 400 MHz



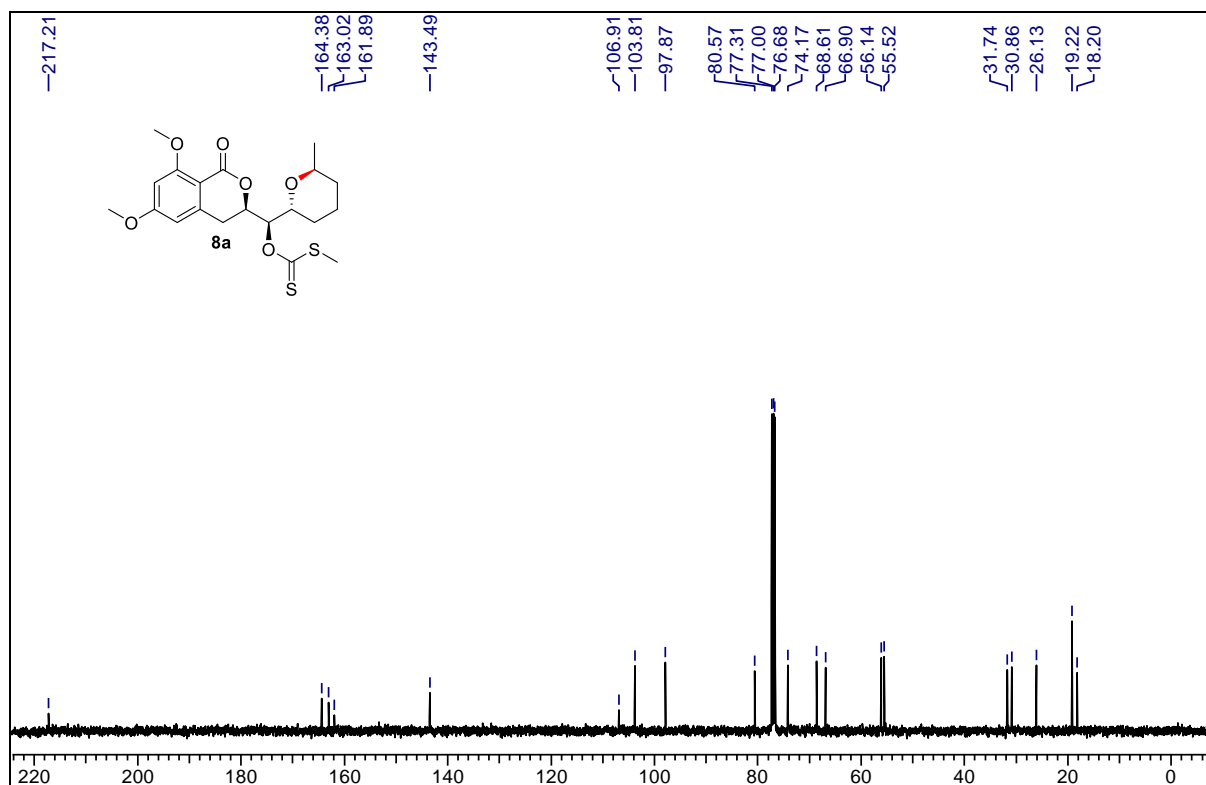
¹³C NMR spectra of compound 7b in 100 MHz



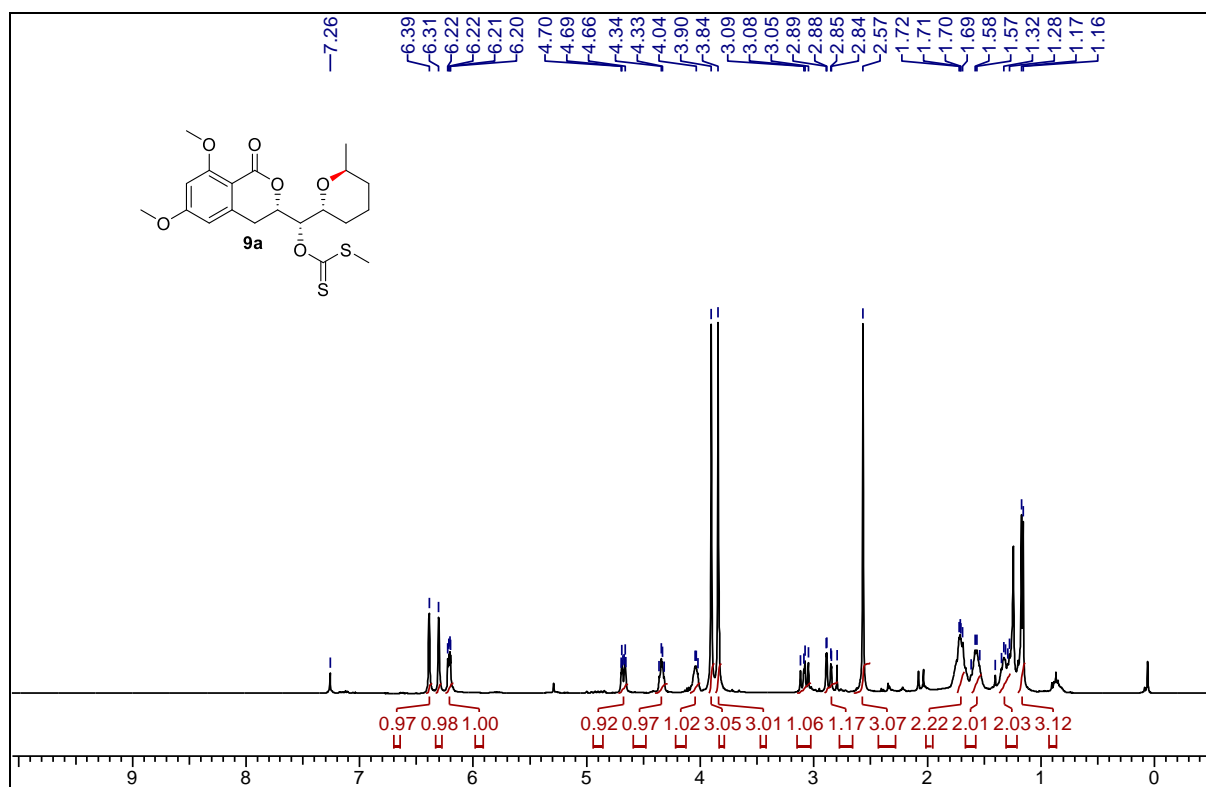
¹H NMR spectra of compound 8a in 400 MHz



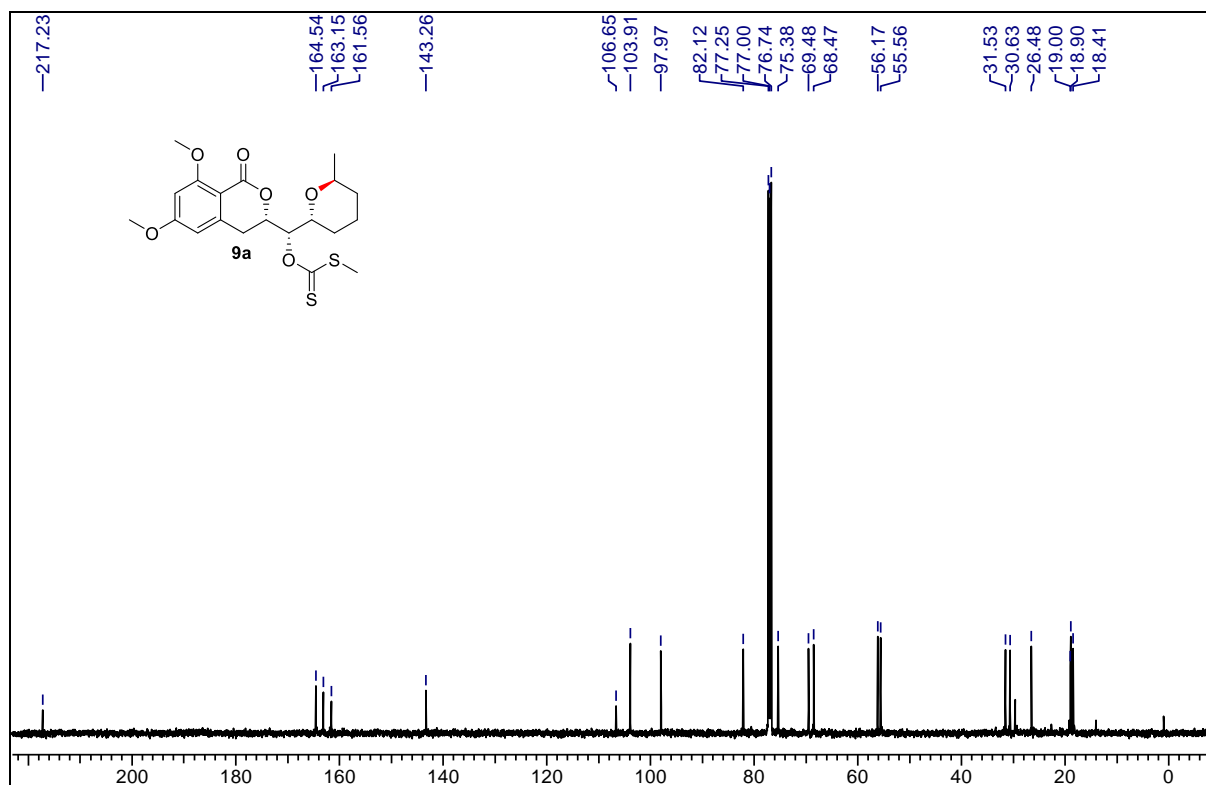
¹³C NMR spectra of compound 8b in 100 MHz



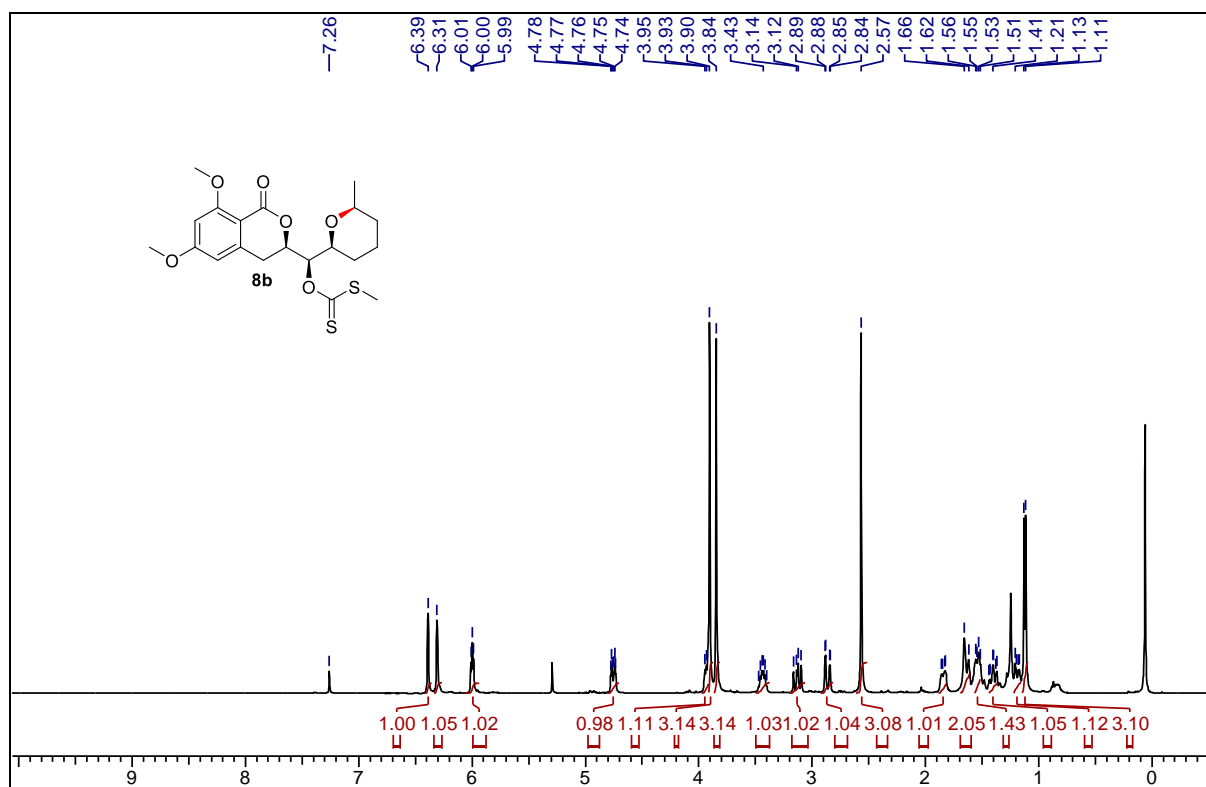
¹H NMR spectra of compound 9a in 400 MHz



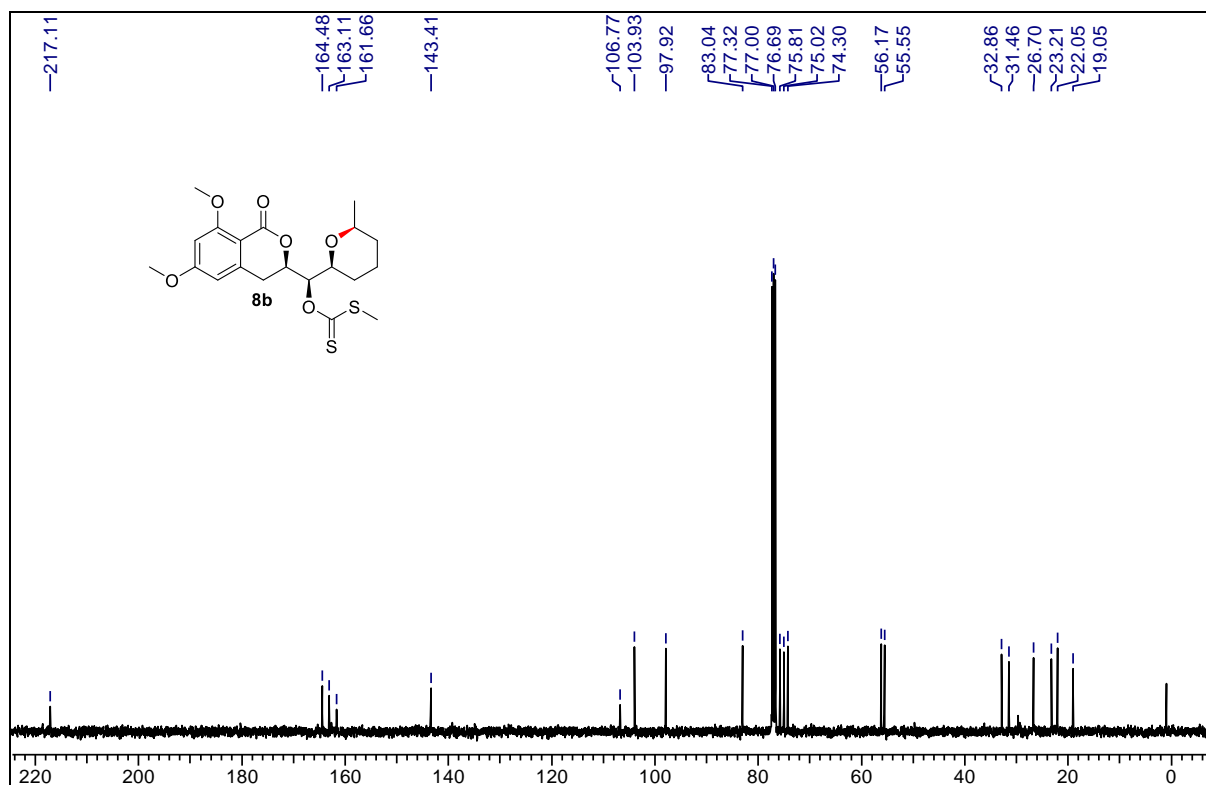
¹³C NMR spectra of compound 9a in 100 MHz



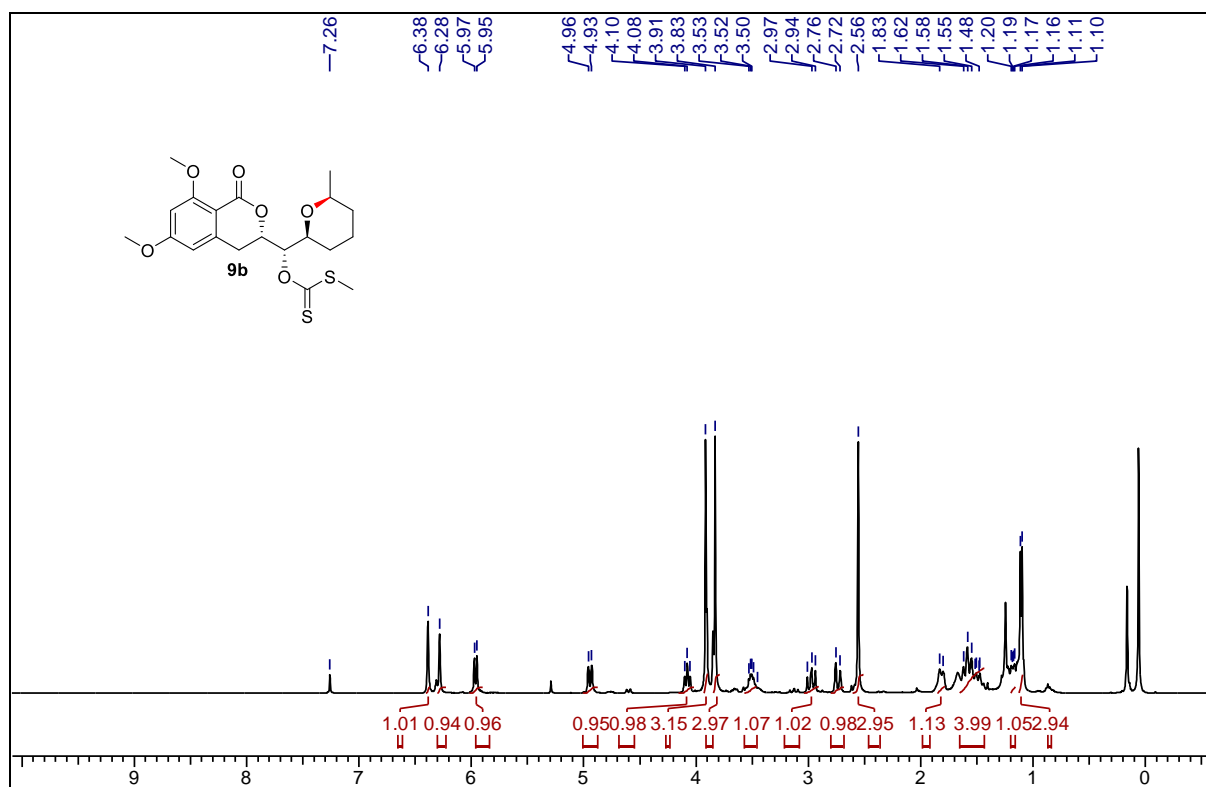
¹H NMR spectra of compound 8b in 400 MHz



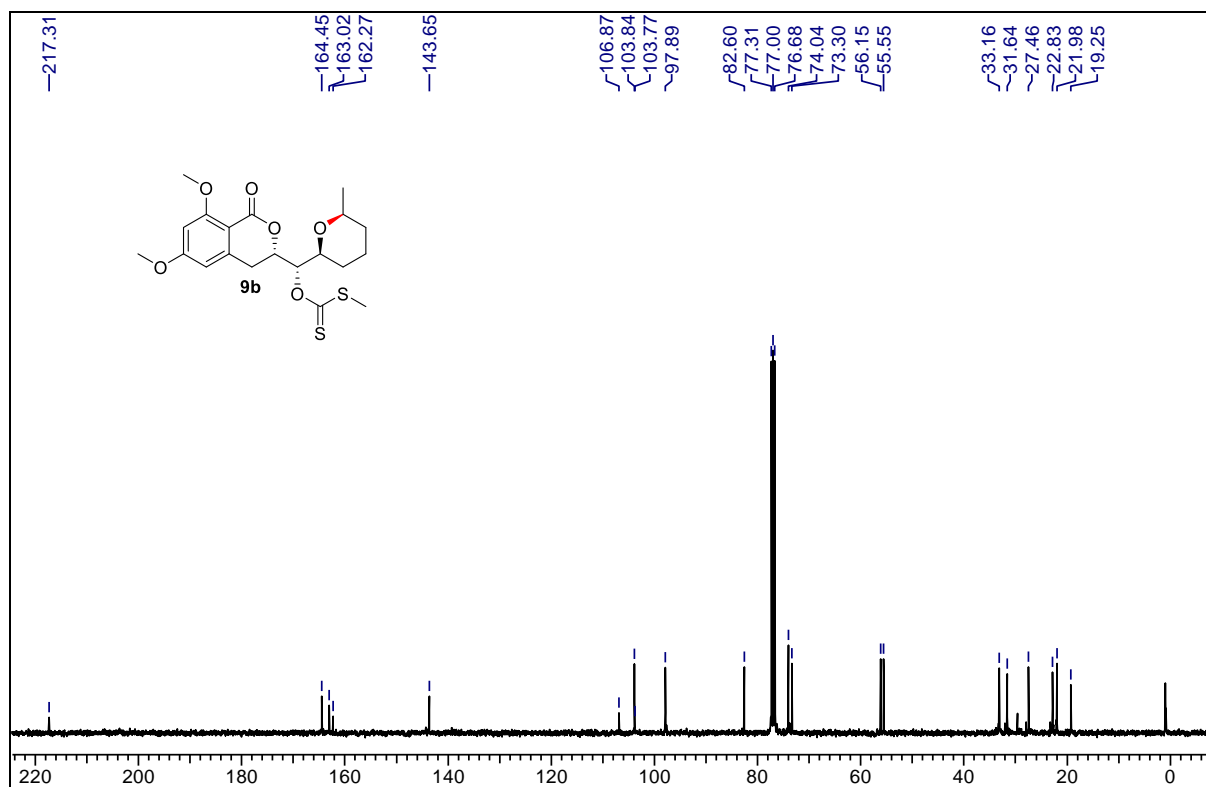
¹³C NMR spectra of compound 8b in 100 MHz



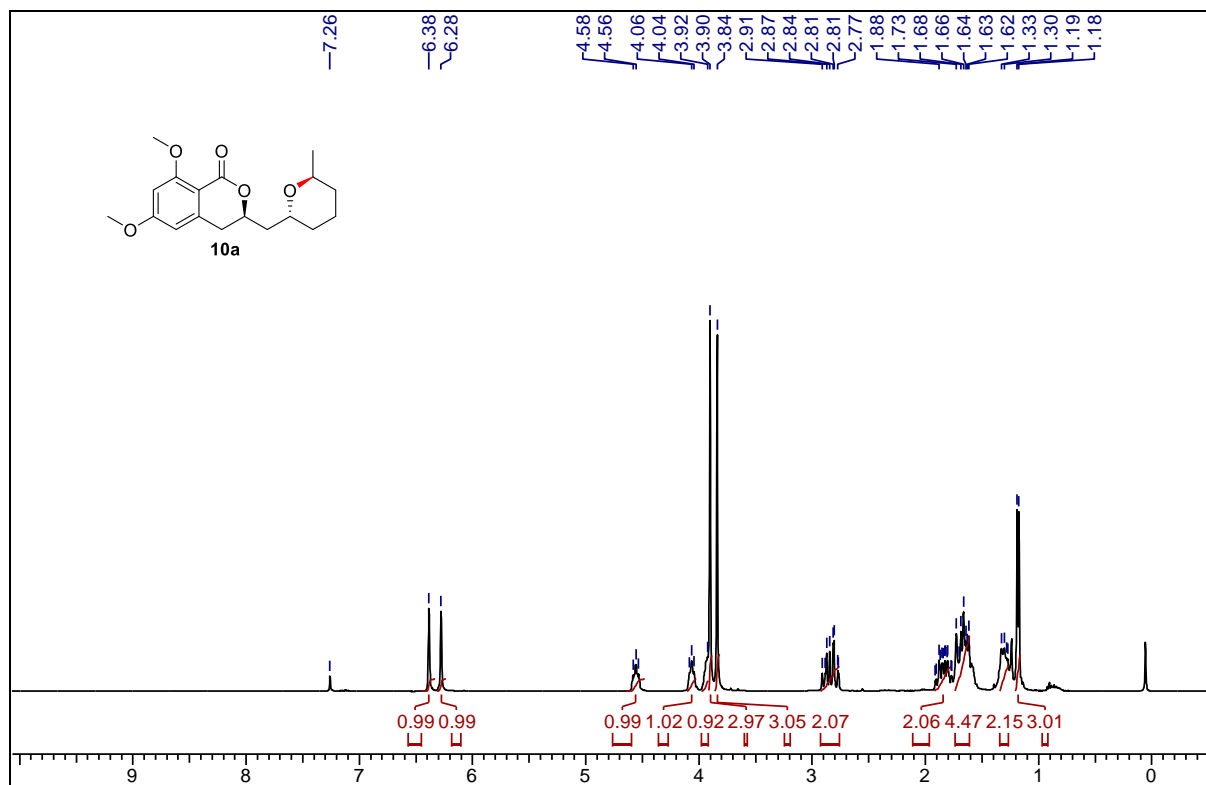
¹H NMR spectra of compound 9b in 400 MHz



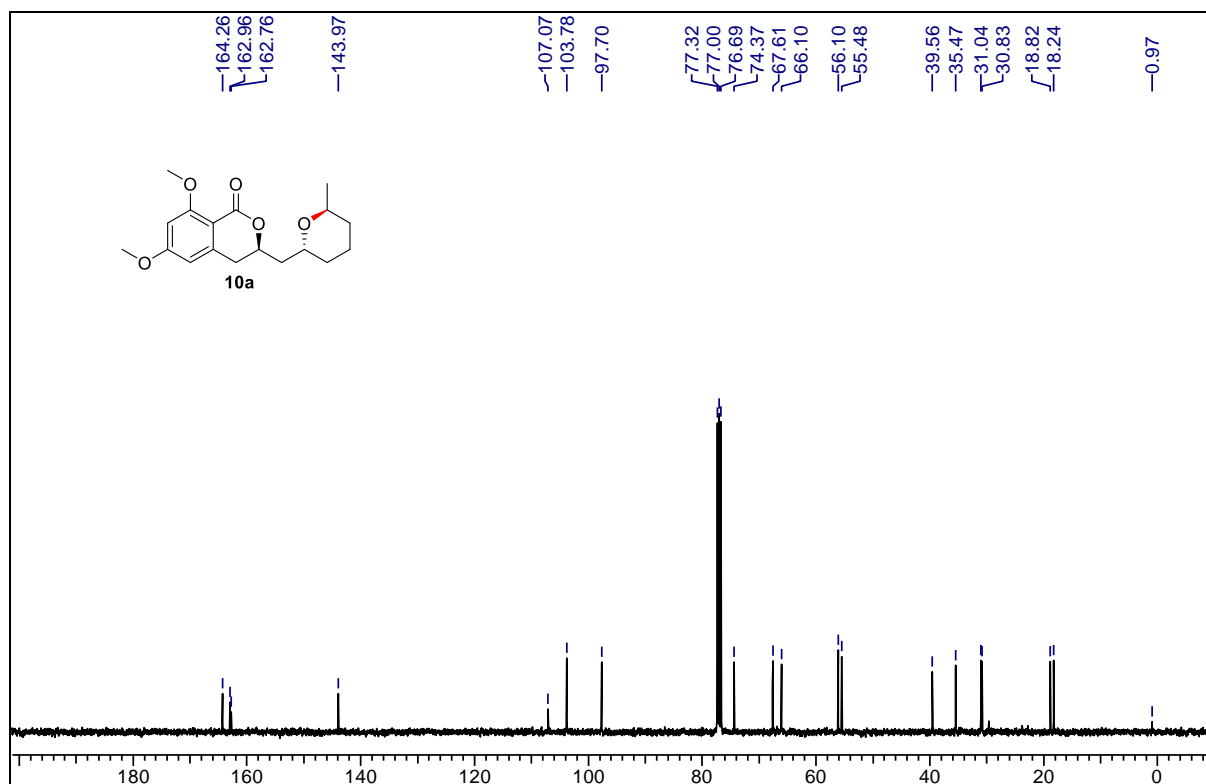
¹³C NMR spectra of compound 9b in 100 MHz



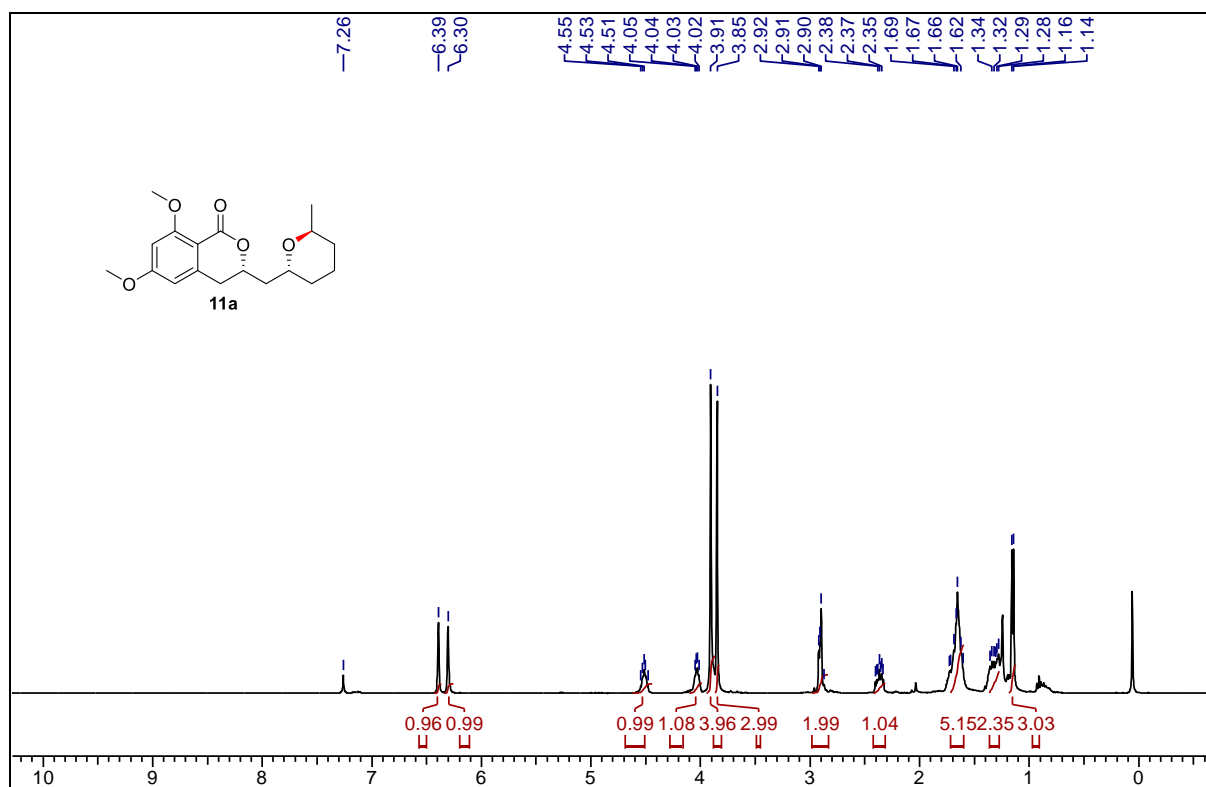
¹H NMR spectra of compound 10a in 400 MHz



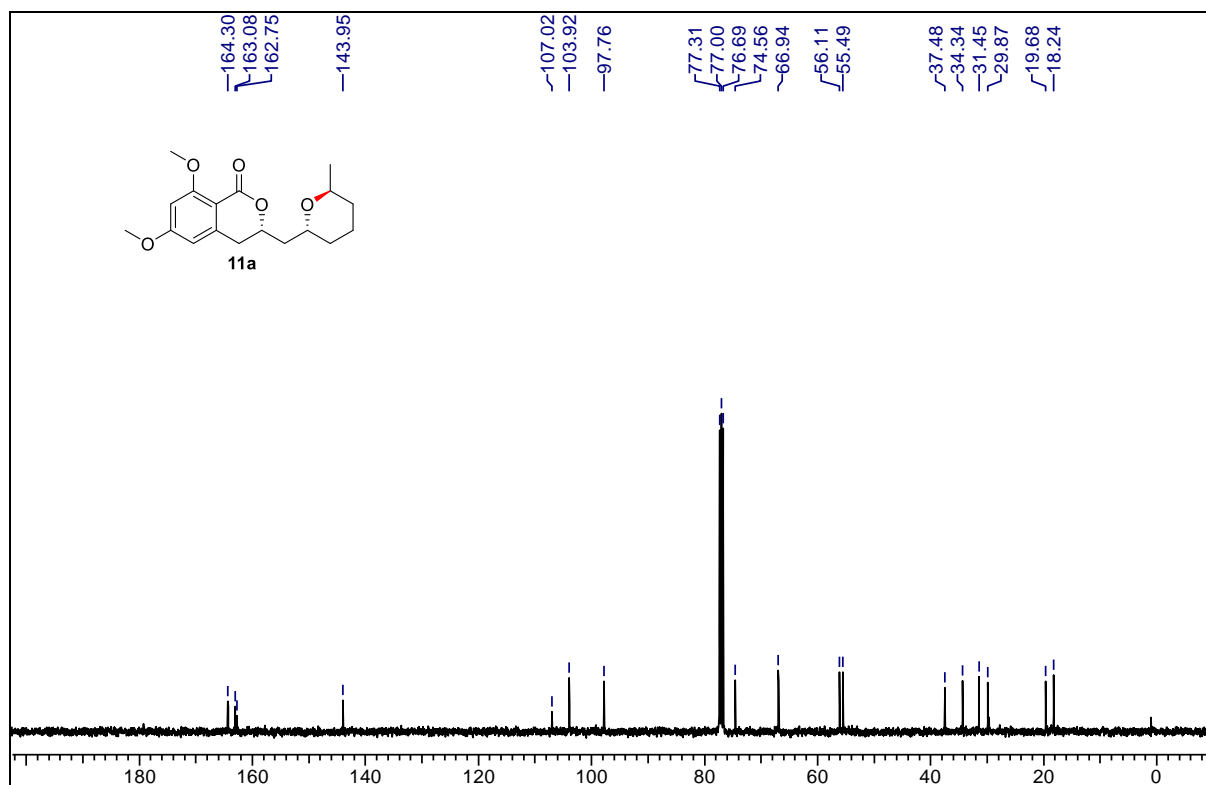
¹³C NMR spectra of compound 10a in 100 MHz



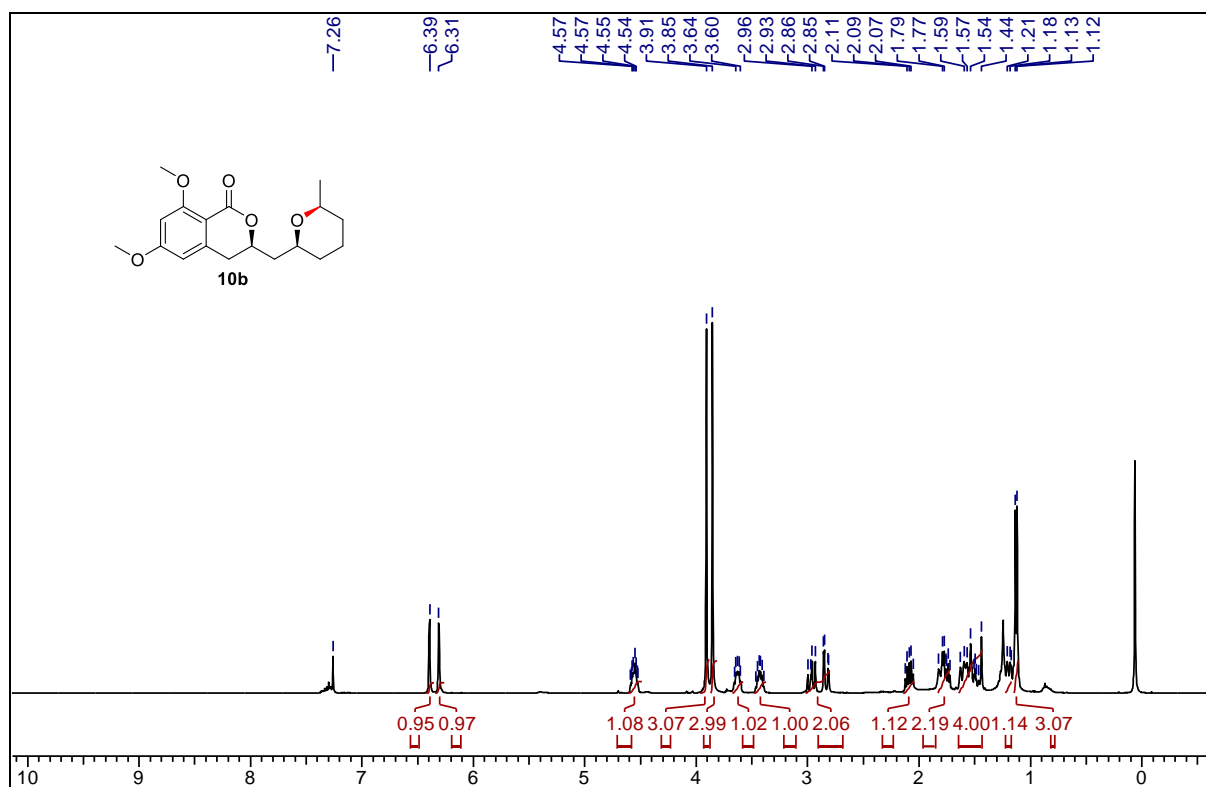
¹H NMR spectra of compound 11a in 400 MHz



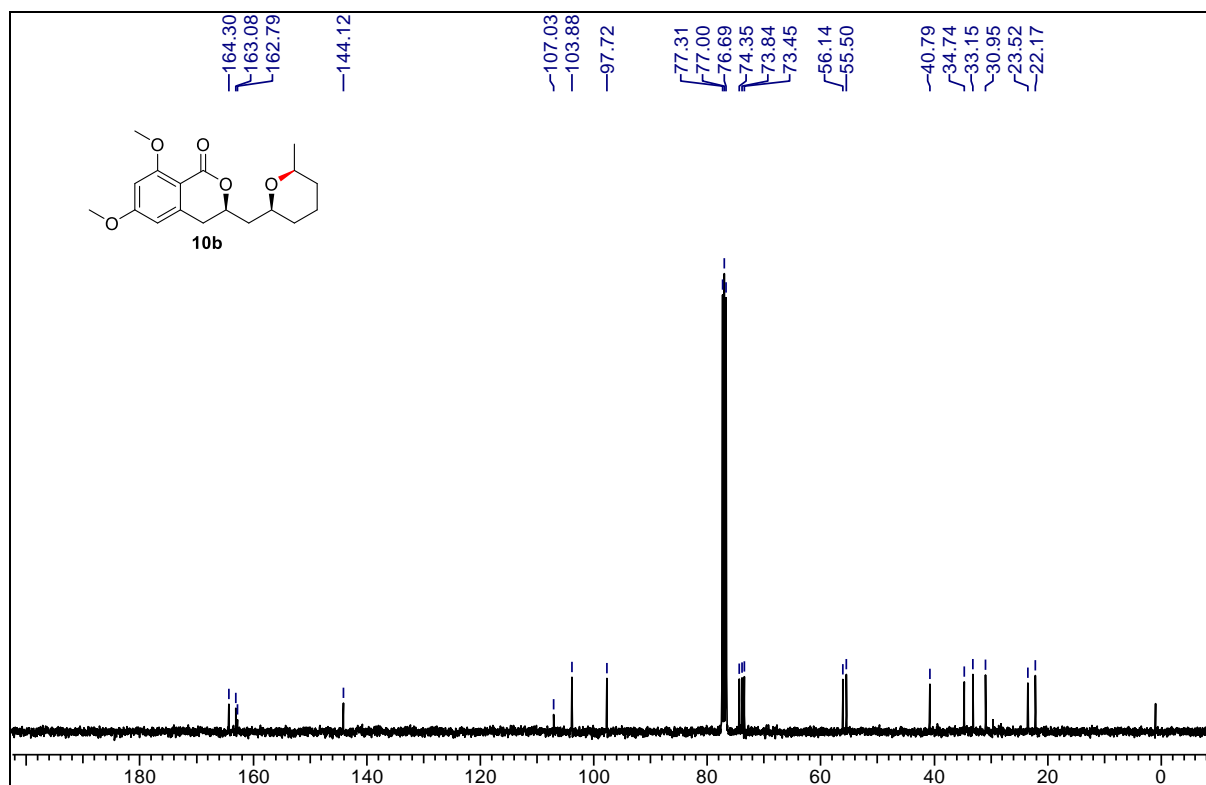
¹³C NMR spectra of compound 11a in 100 MHz



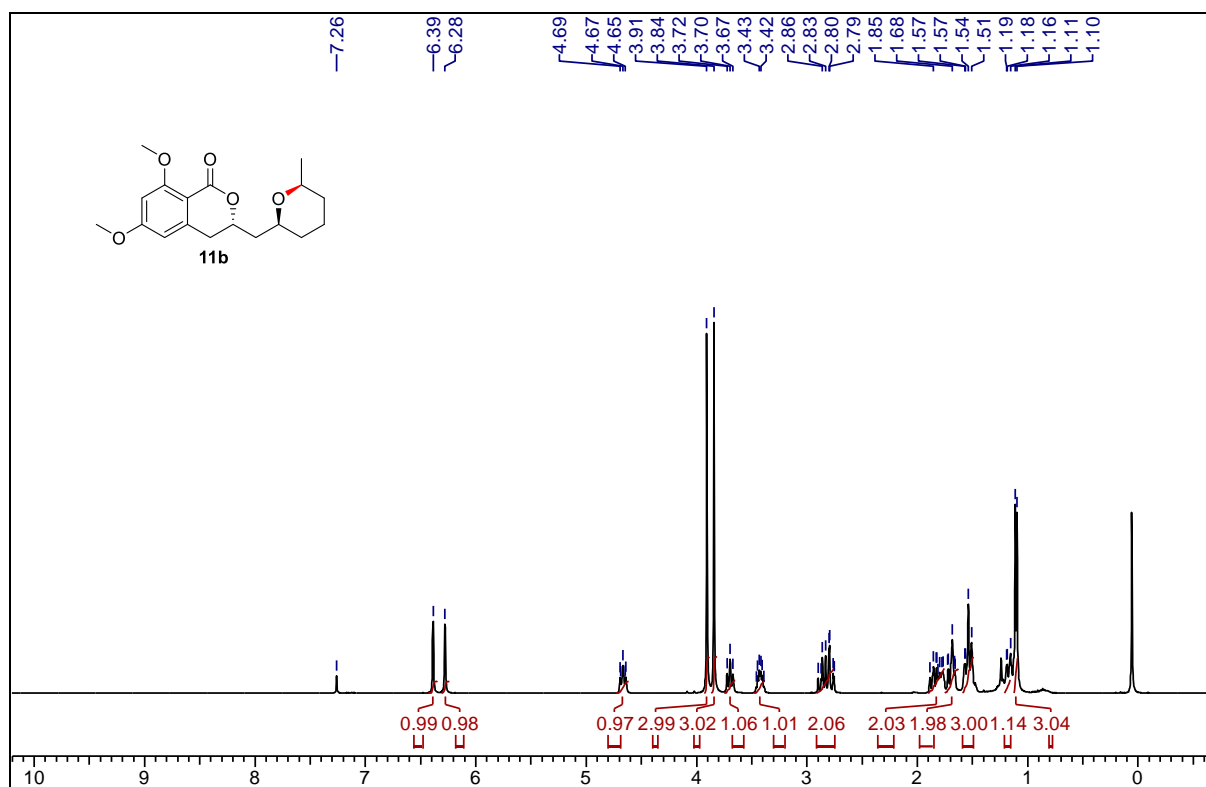
^1H NMR spectra of compound 10b in 400 MHz



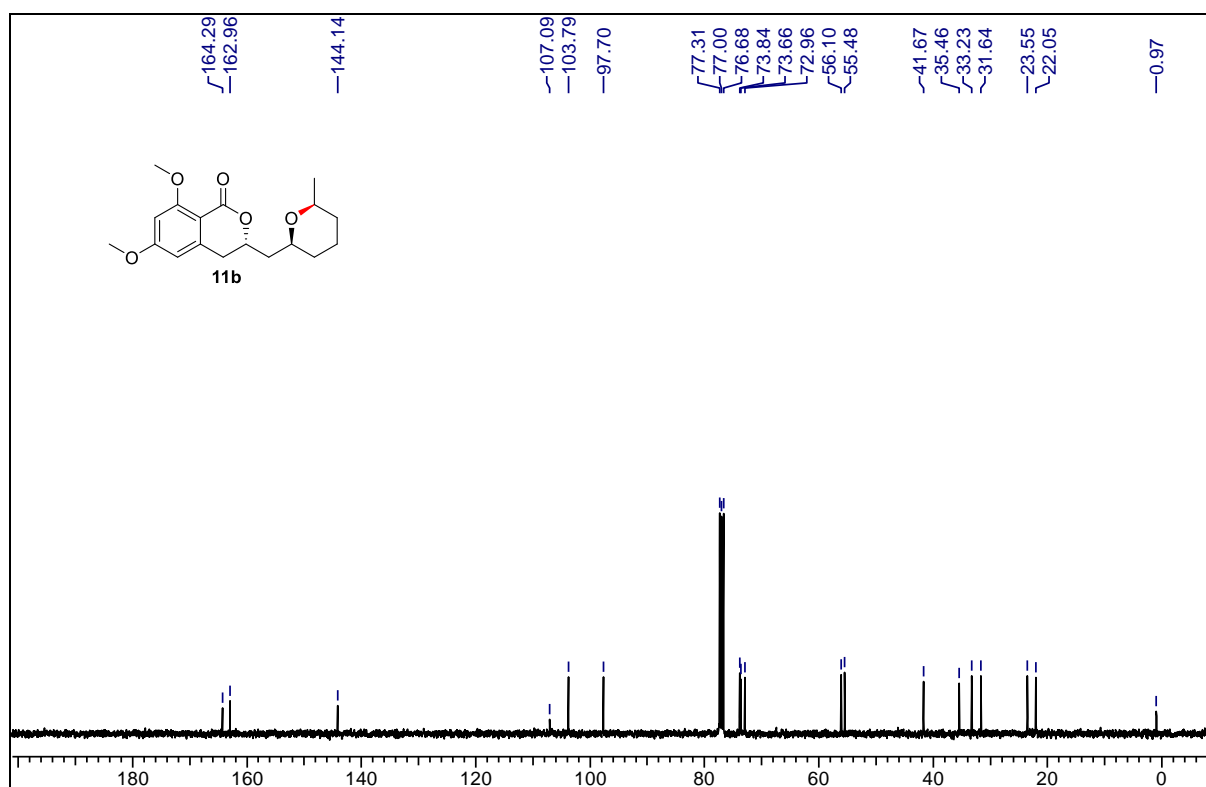
^{13}C NMR spectra of compound 10b in 100 MHz



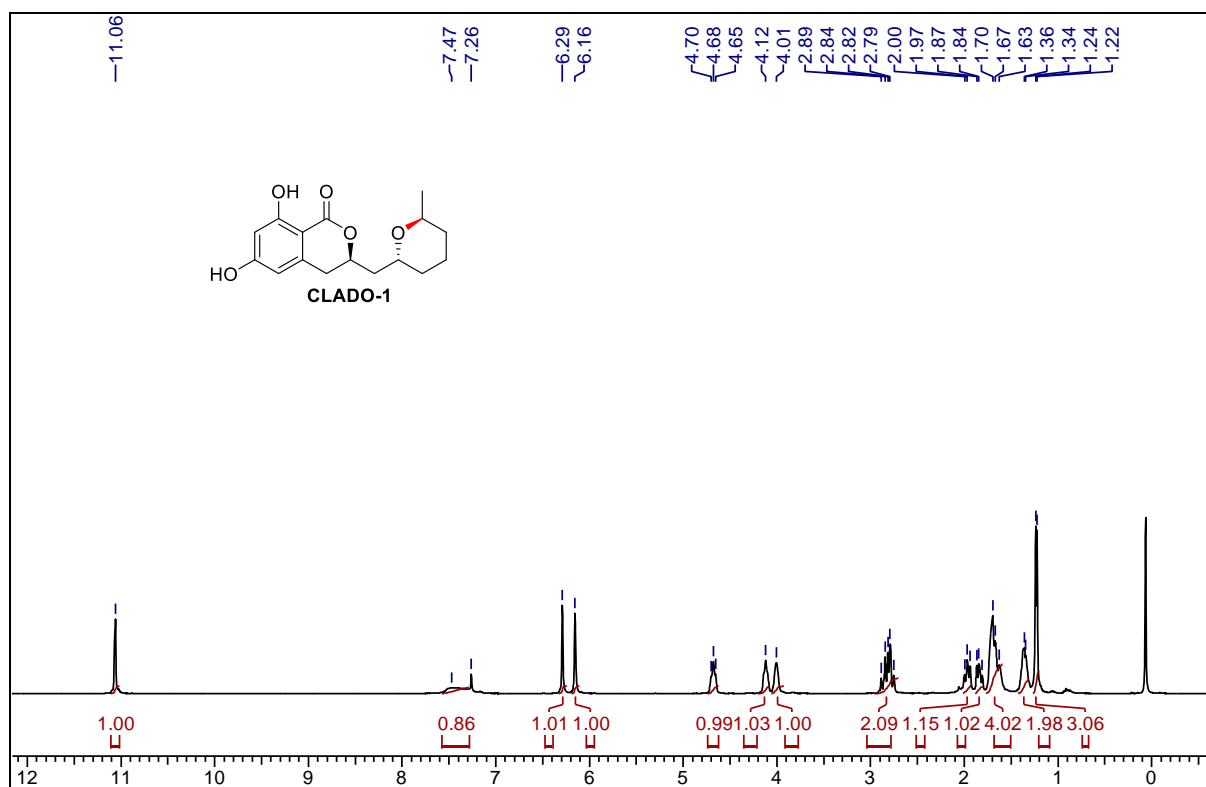
¹H NMR spectra of compound 11b in 400 MHz



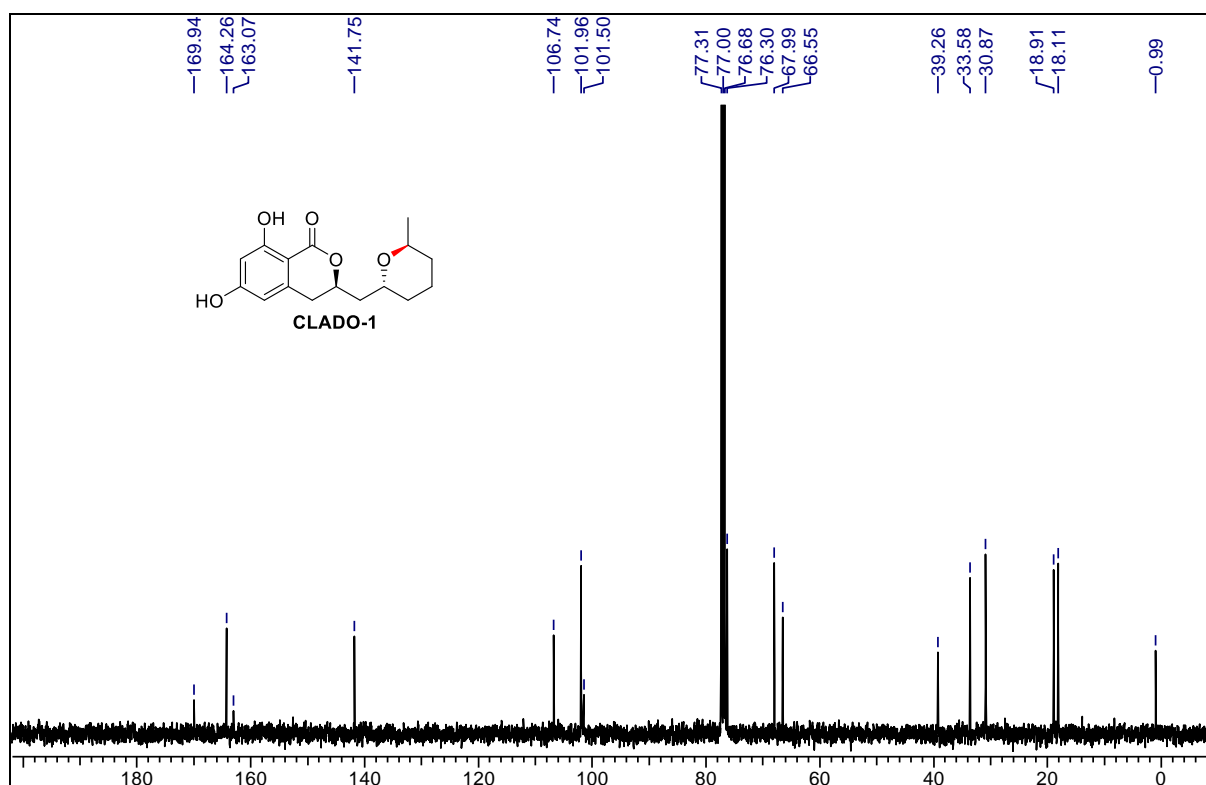
¹³C NMR spectra of compound 11b in 100 MHz



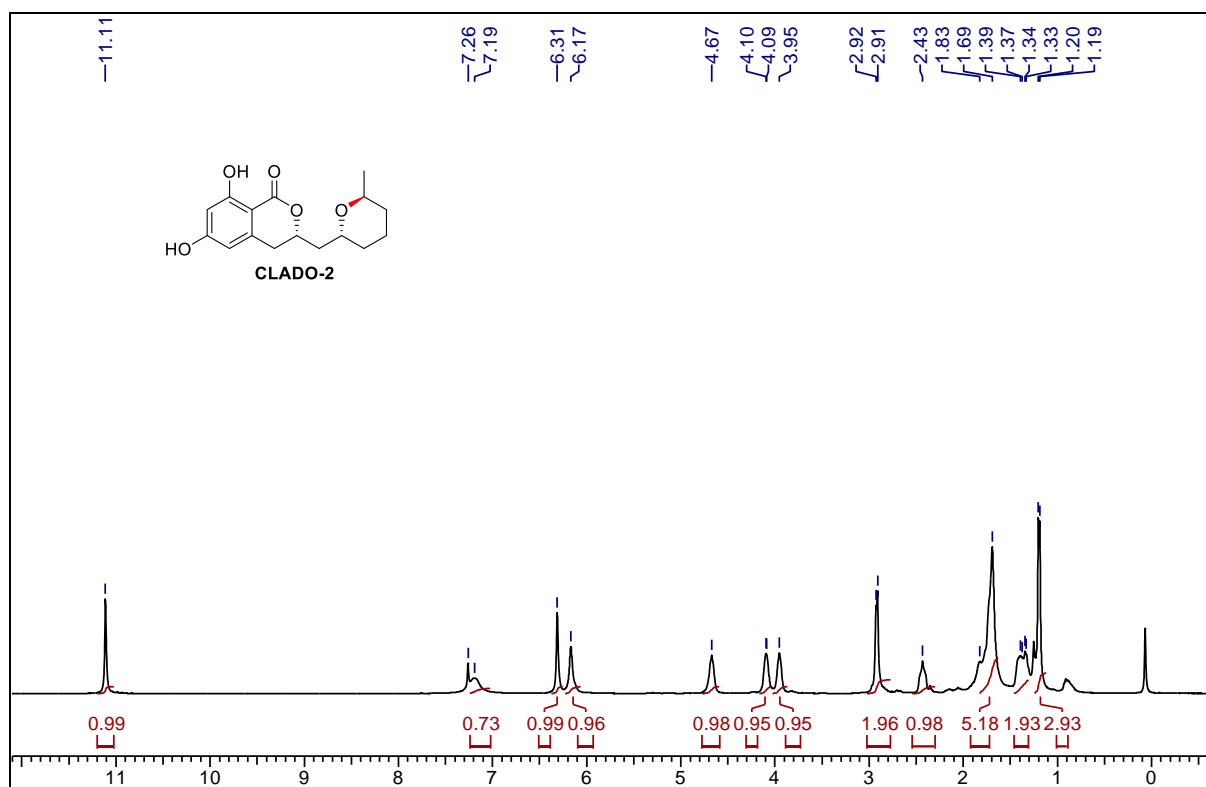
^1H NMR of Cladosporin (12) in 400 MHz



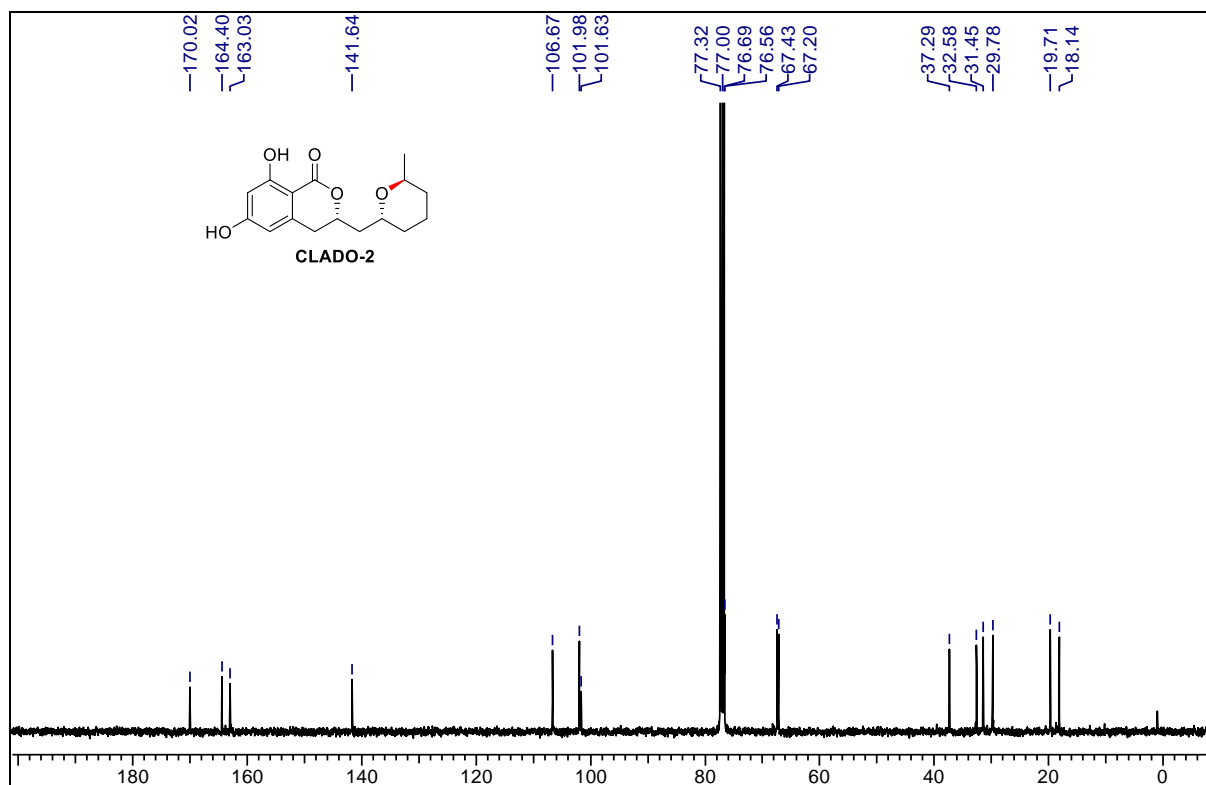
^{13}C NMR of Cladosporin (12) in 100 MHz



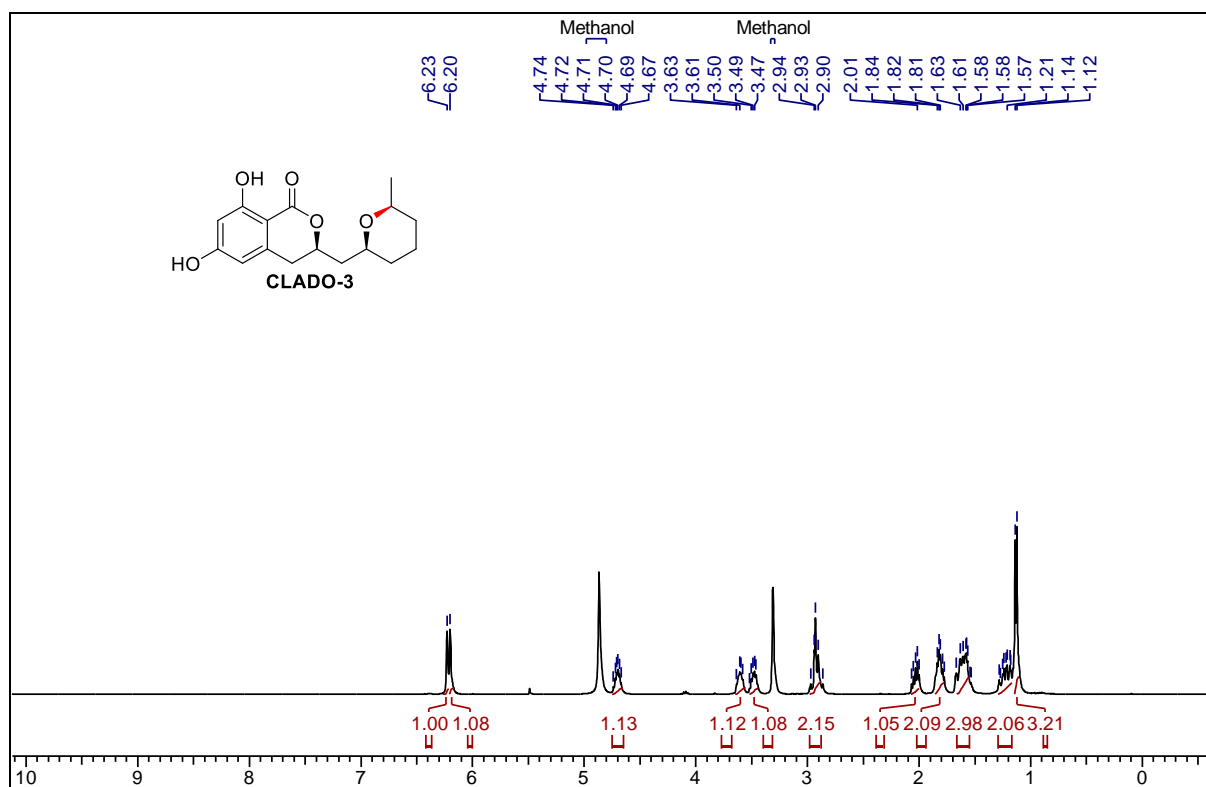
^1H NMR spectra of compound 13 in 400 MHz



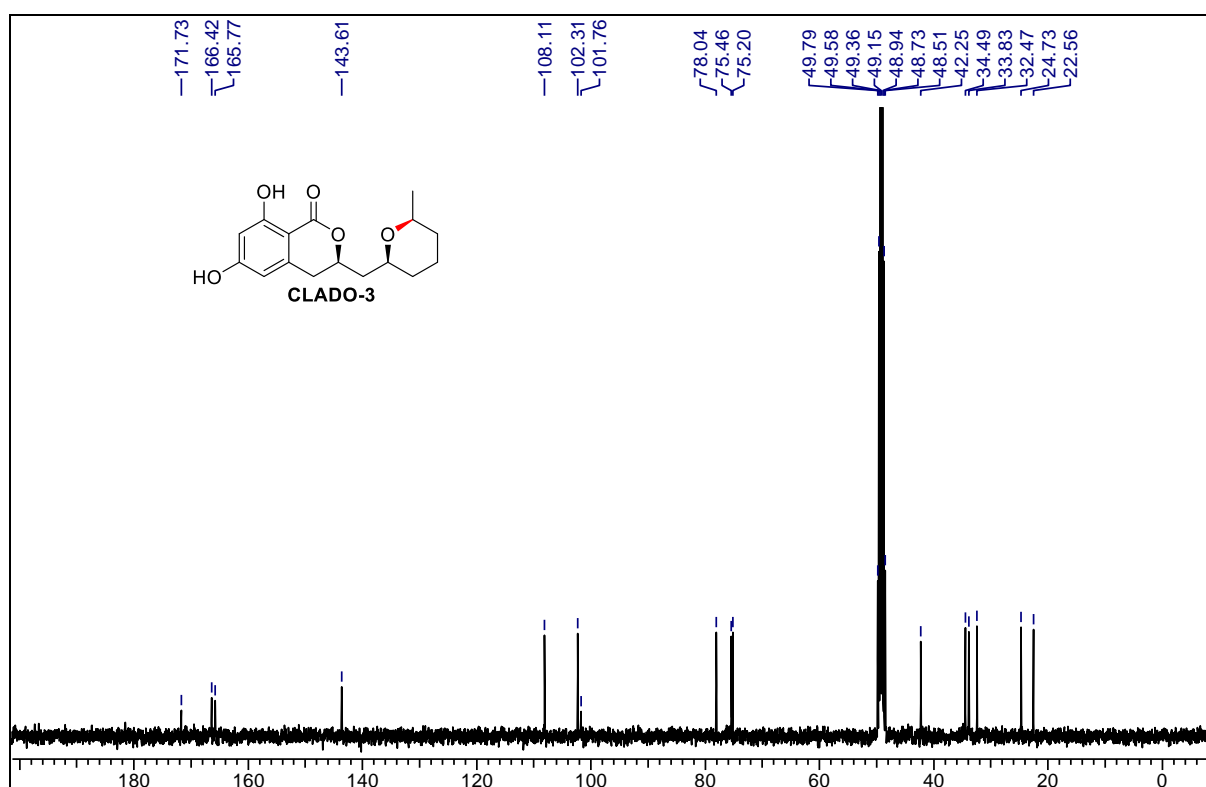
^{13}C NMR ^1H NMR spectra of compound 13 in 100 MHz



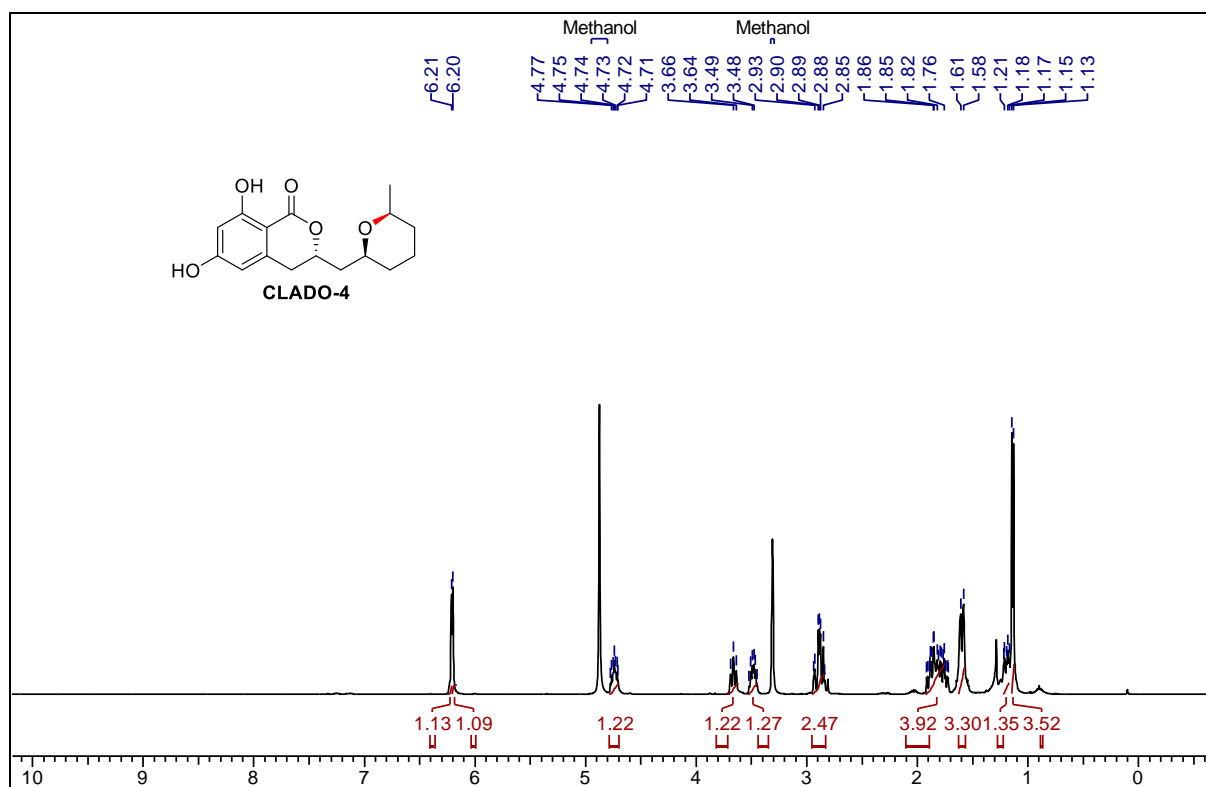
^1H NMR spectra of compound 14 in 400 MHz



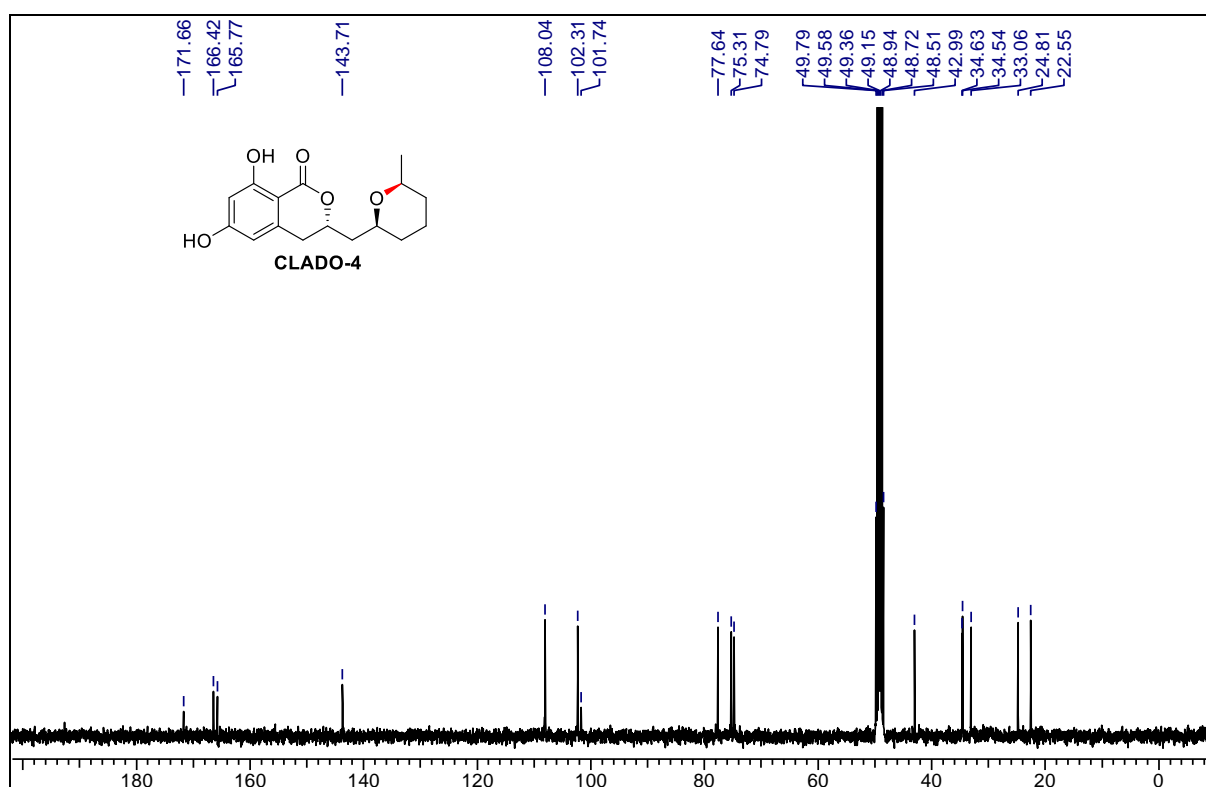
^{13}C NMR spectra of compound 14 in 100 MHz



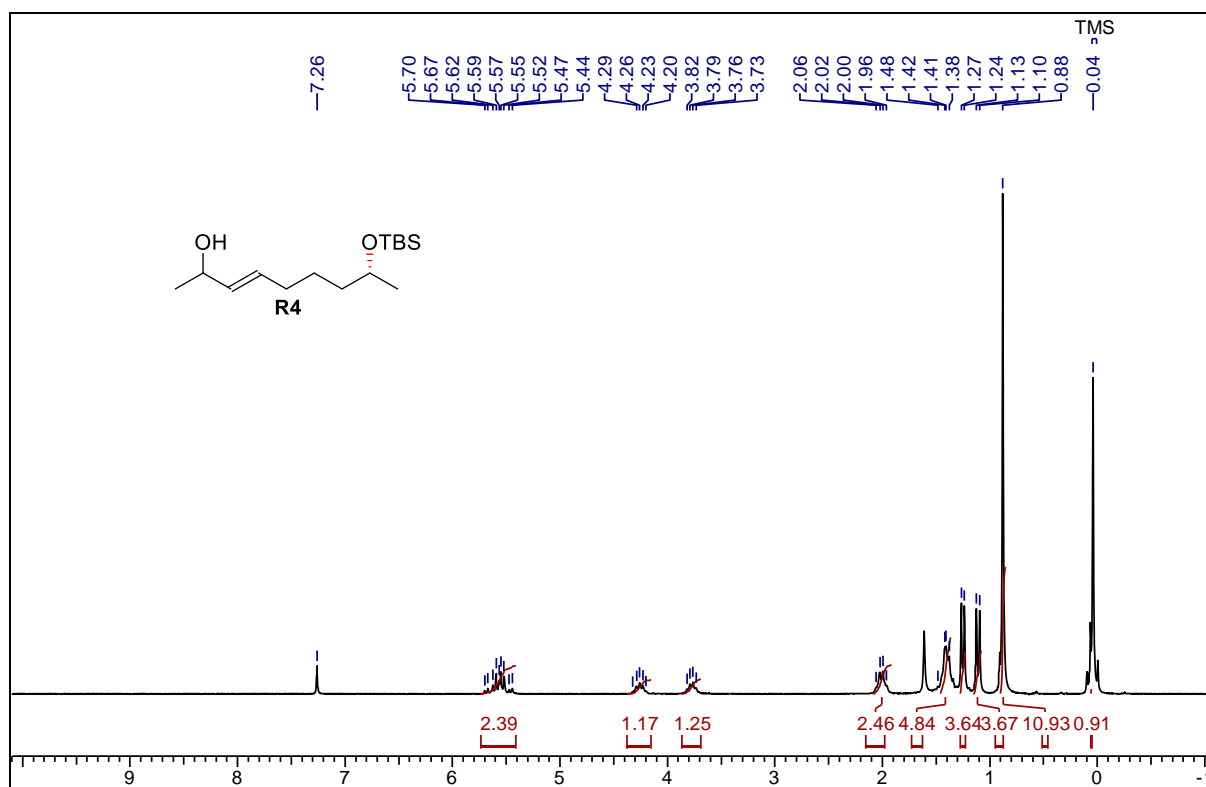
^1H NMR spectra of compound 15 in 400 MHz



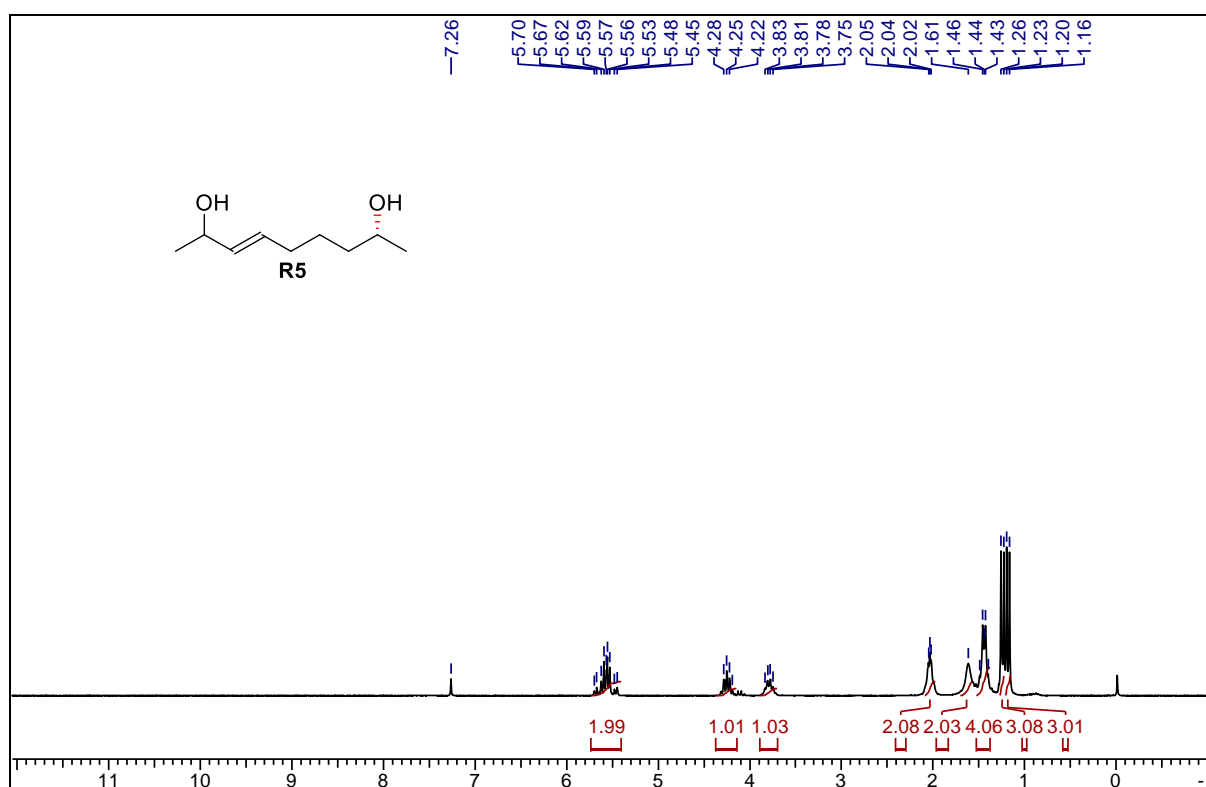
^{13}C NMR spectra of compound 15 in 100 MHz



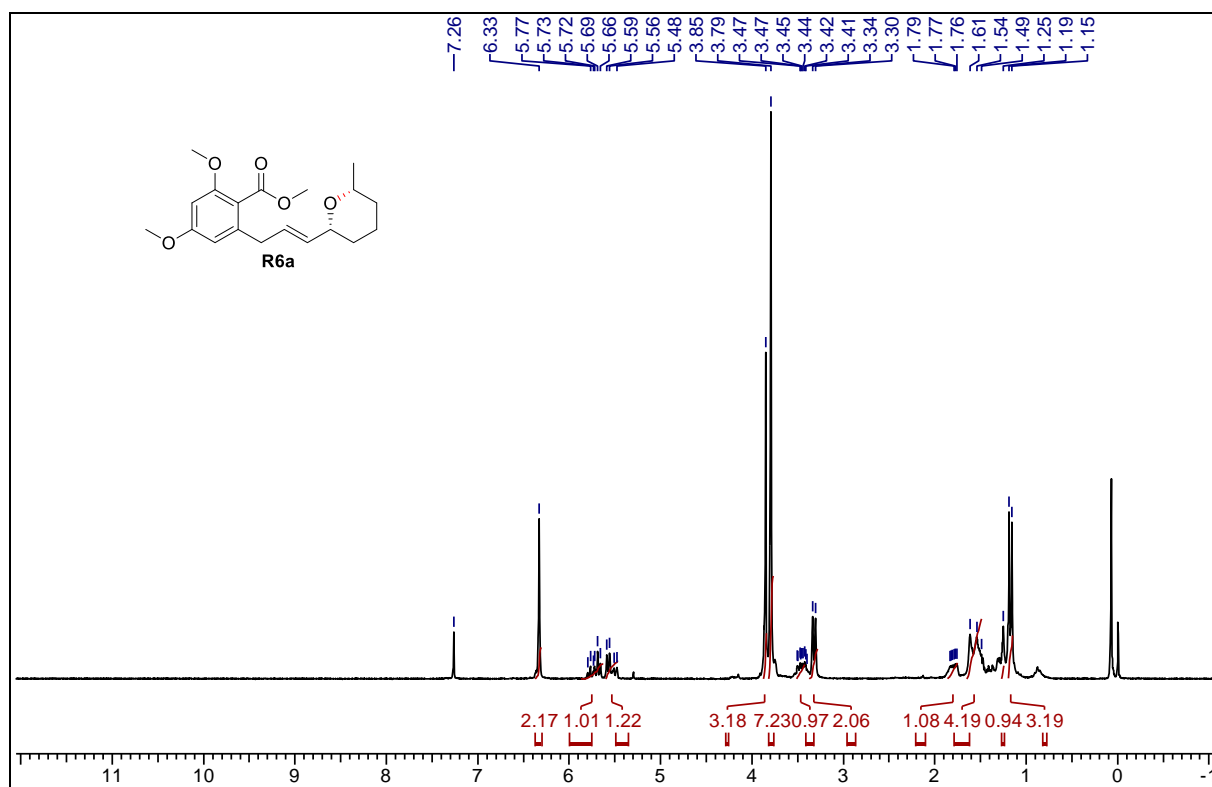
^1H NMR spectra of compound R4 in 400 MHz



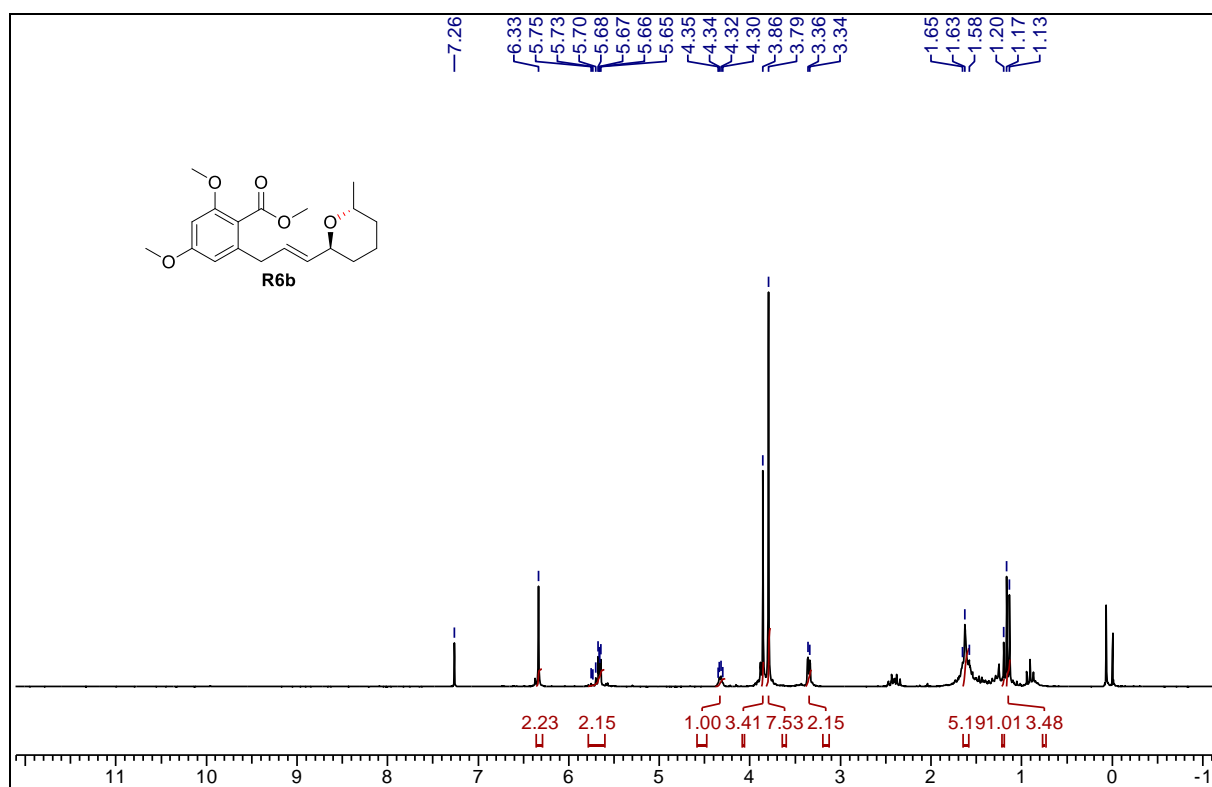
^1H NMR spectra of compound R5 in 400 MHz



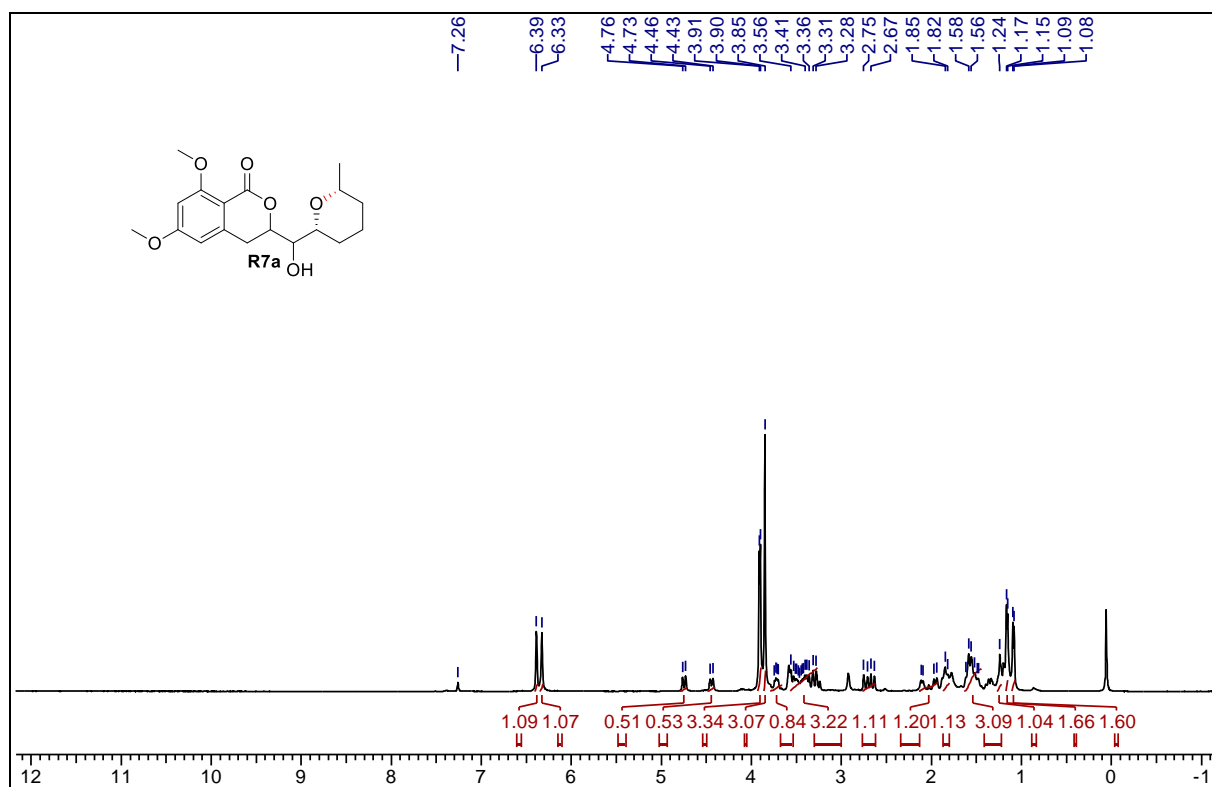
^1H NMR spectra of compound R6a in 400 MHz



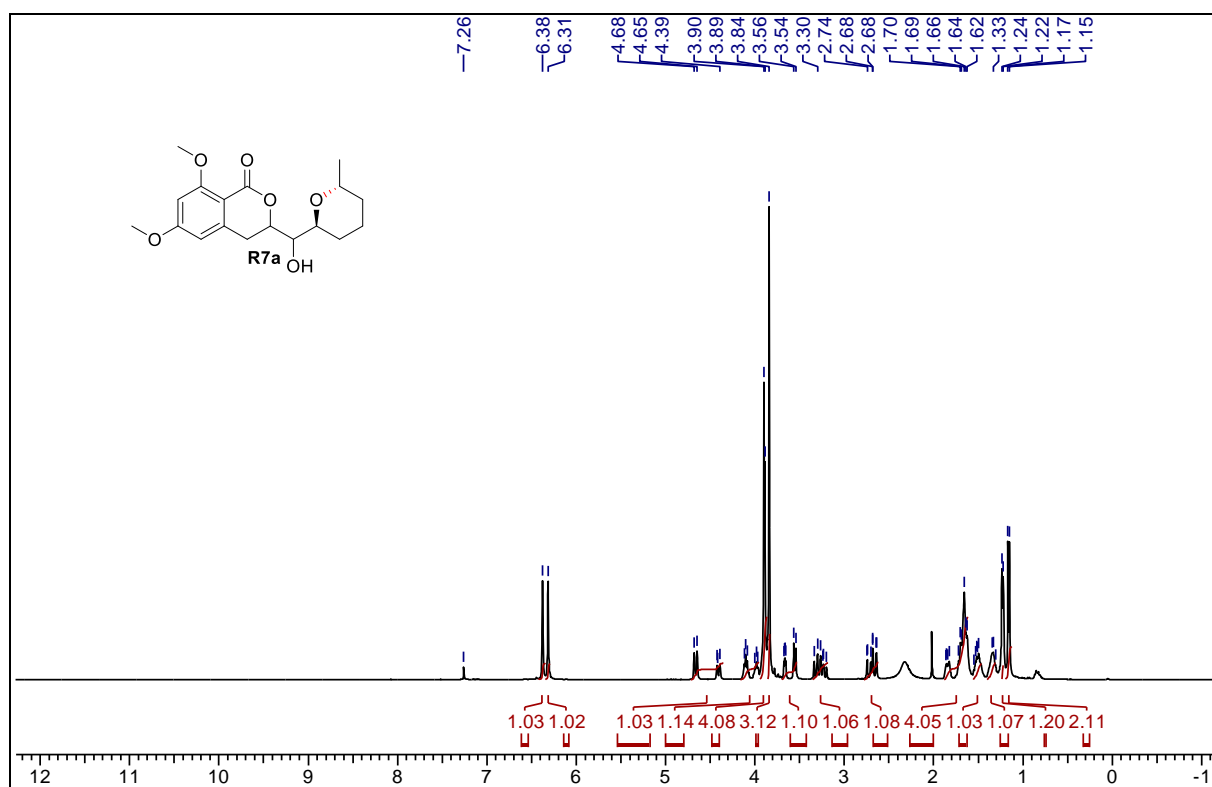
^1H NMR spectra of compound R6b in 400 MHz



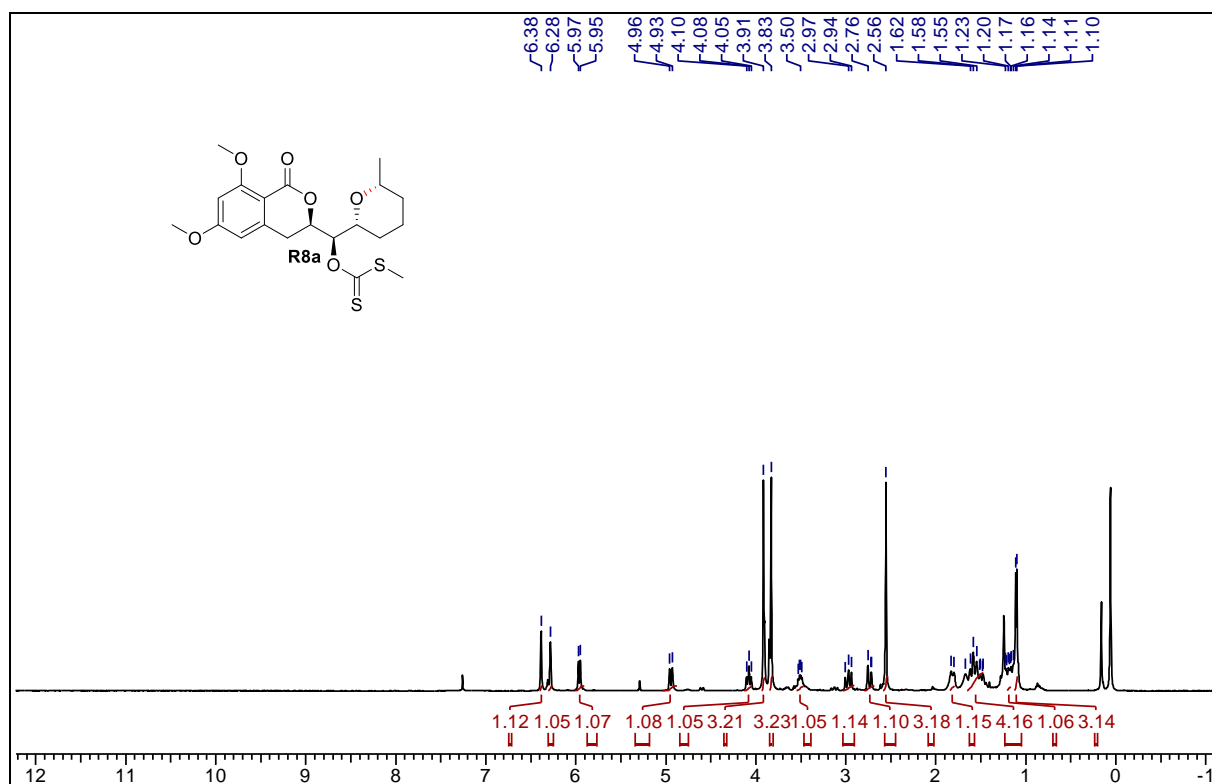
¹H NMR spectra of compound R7a in 400 MHz



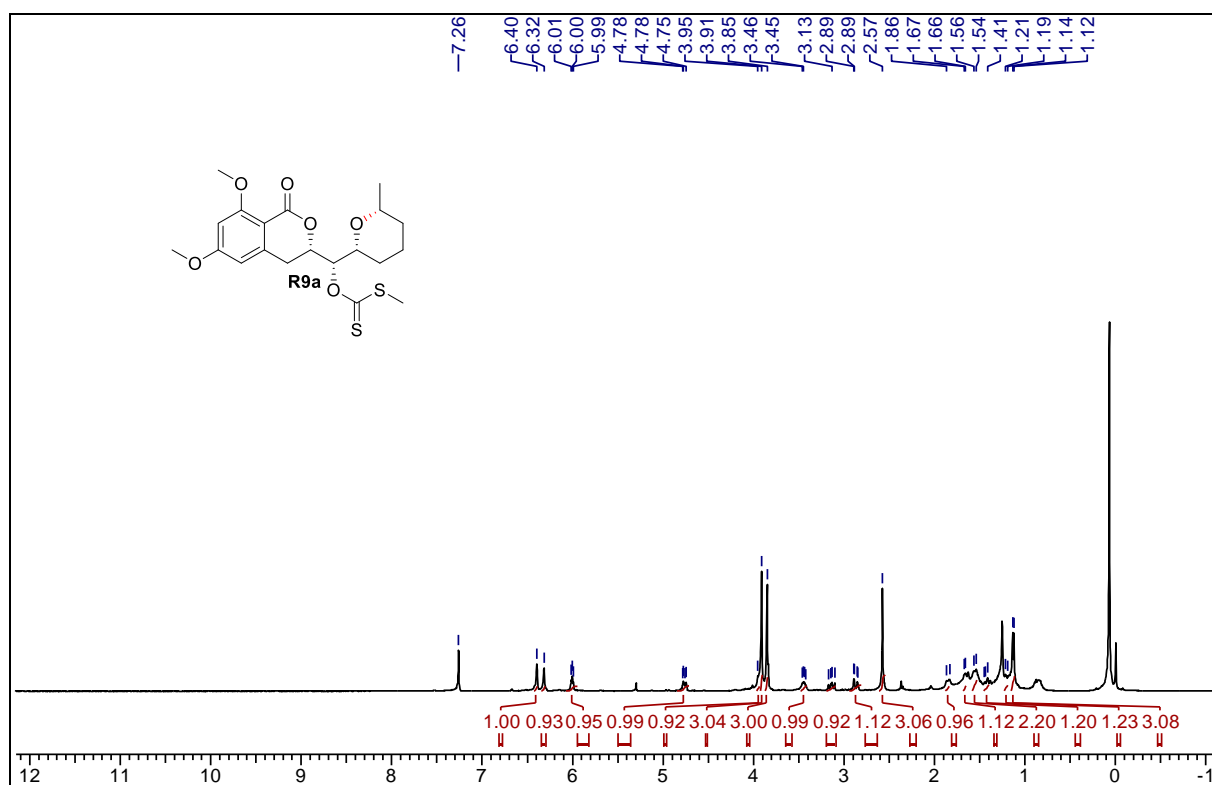
¹H NMR spectra of compound R7b in 400 MHz



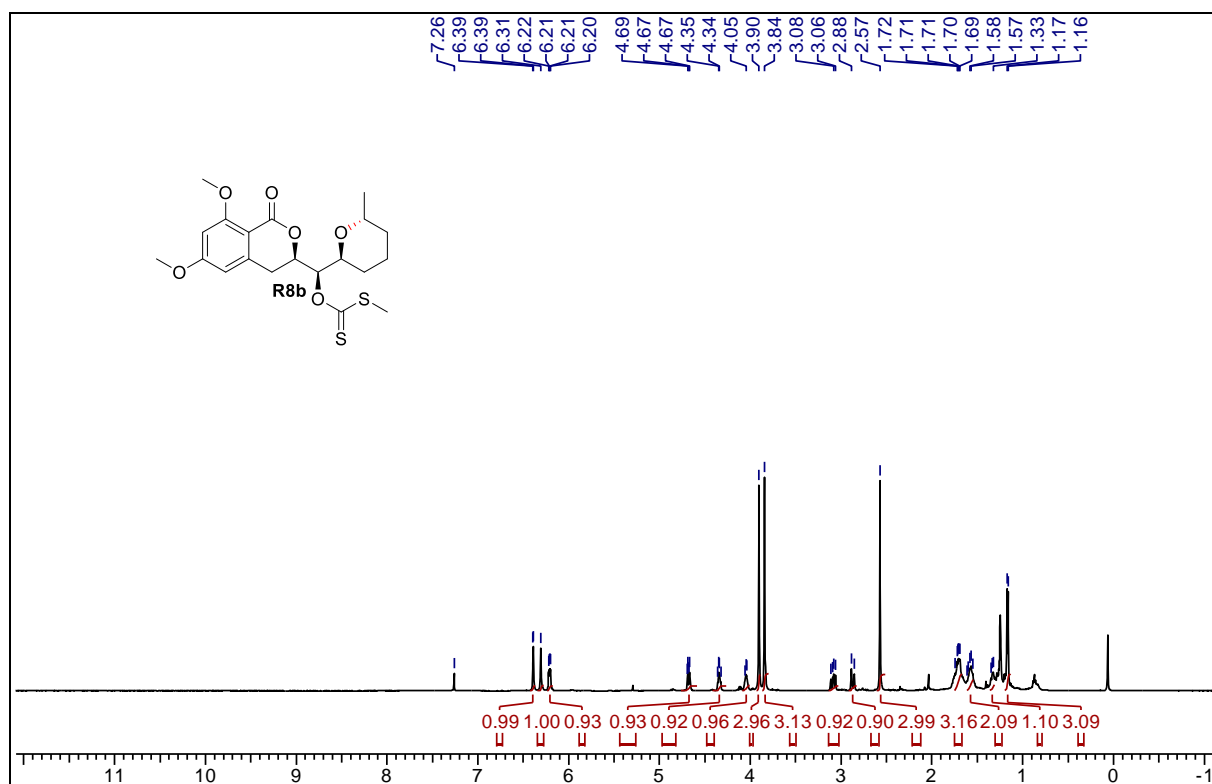
¹H NMR spectra of compound R8a in 400 MHz



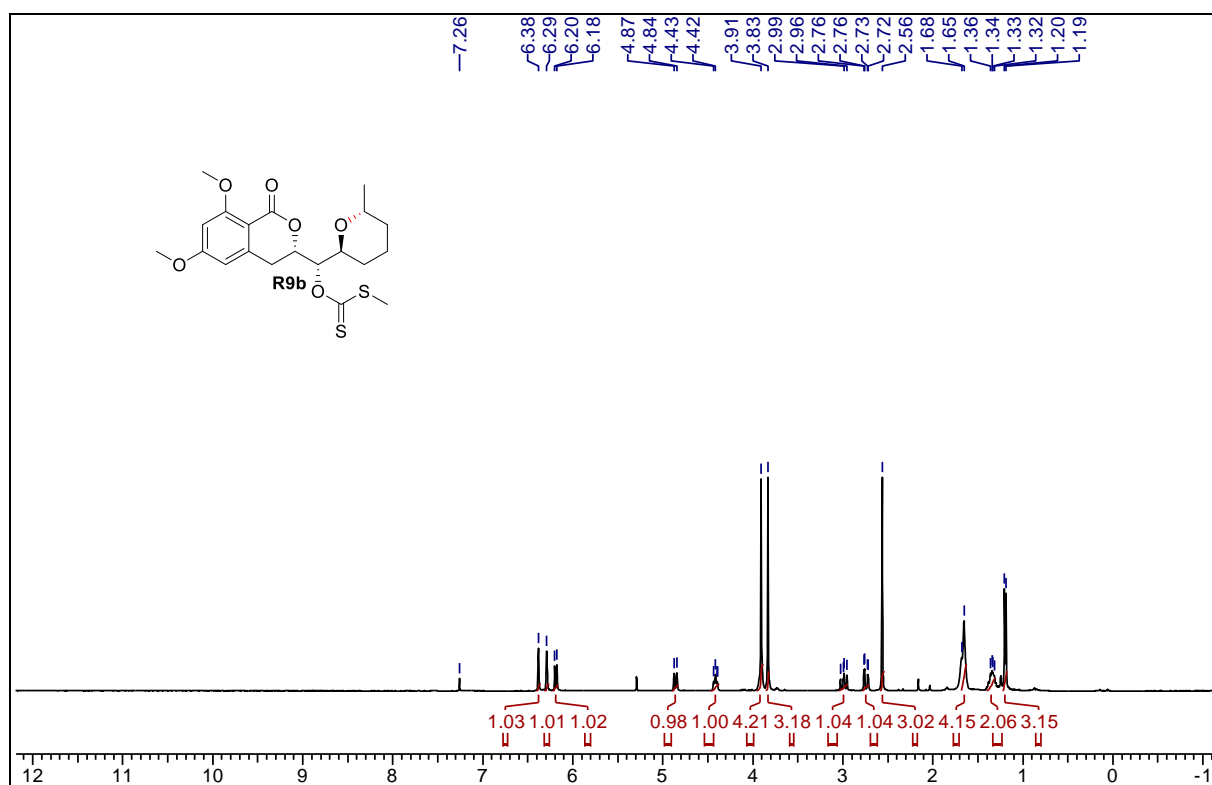
¹H NMR spectra of compound R9a in 400 MHz



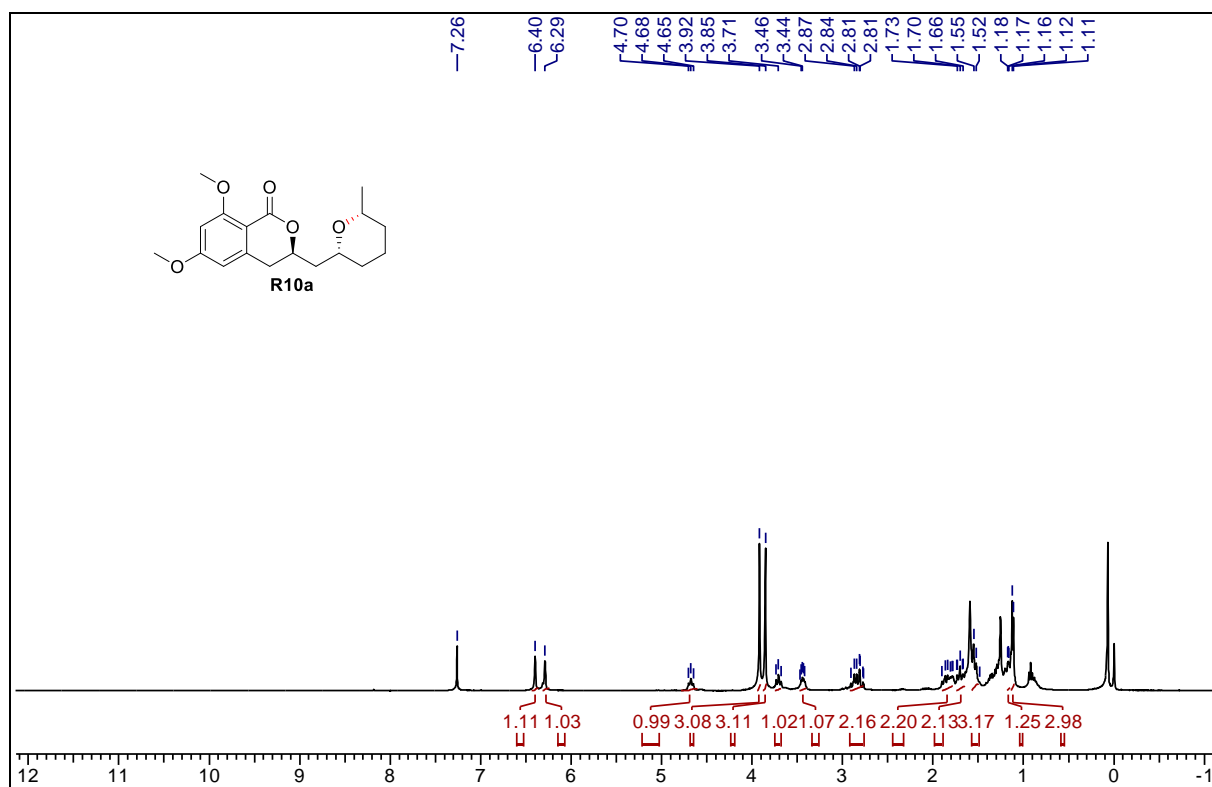
¹H NMR spectra of compound R8b in 400 MHz



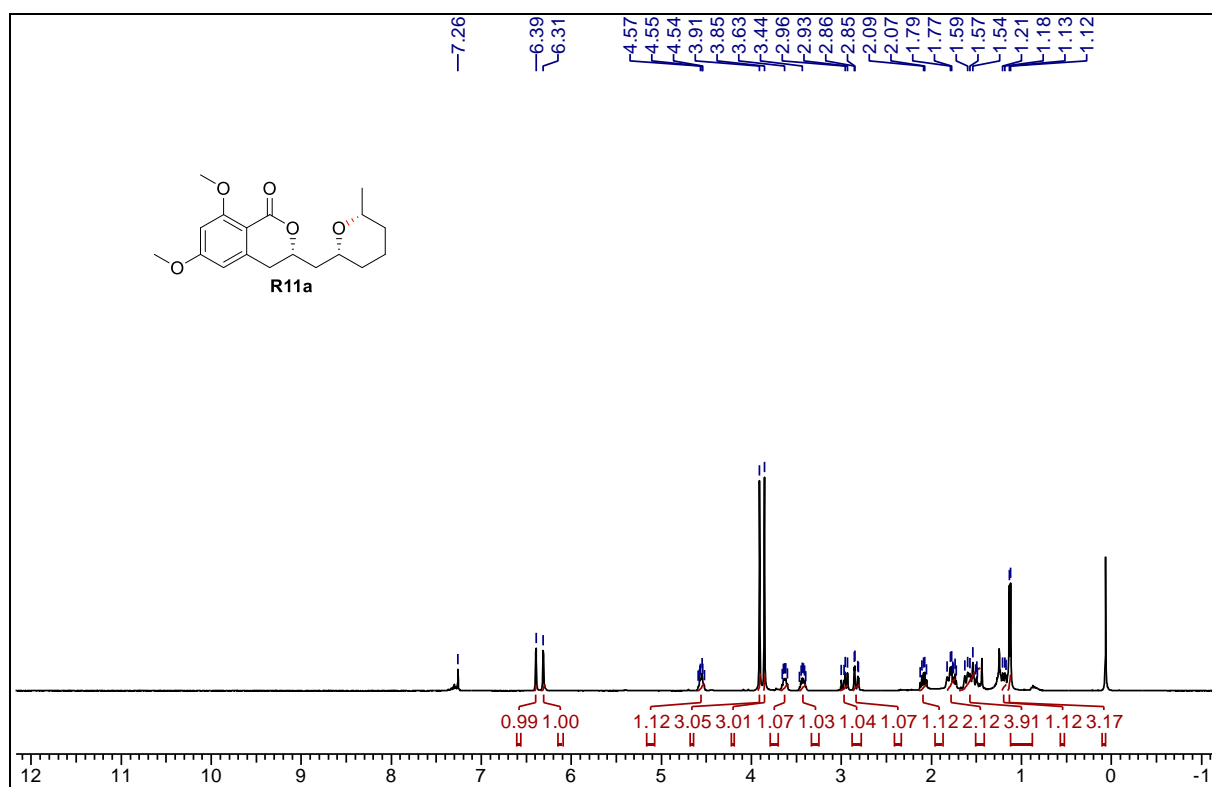
¹H NMR spectra of compound R9b in 400 MHz



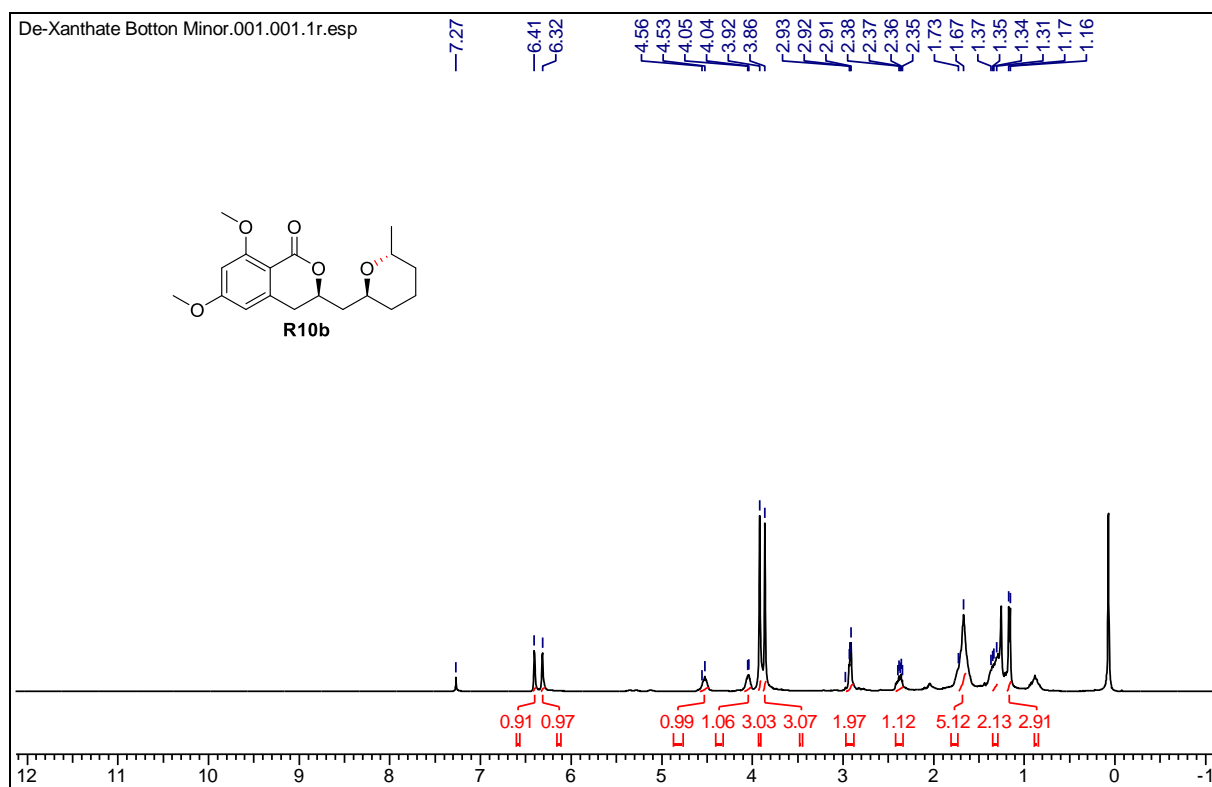
¹H NMR spectra of compound R10a in 400 MHz



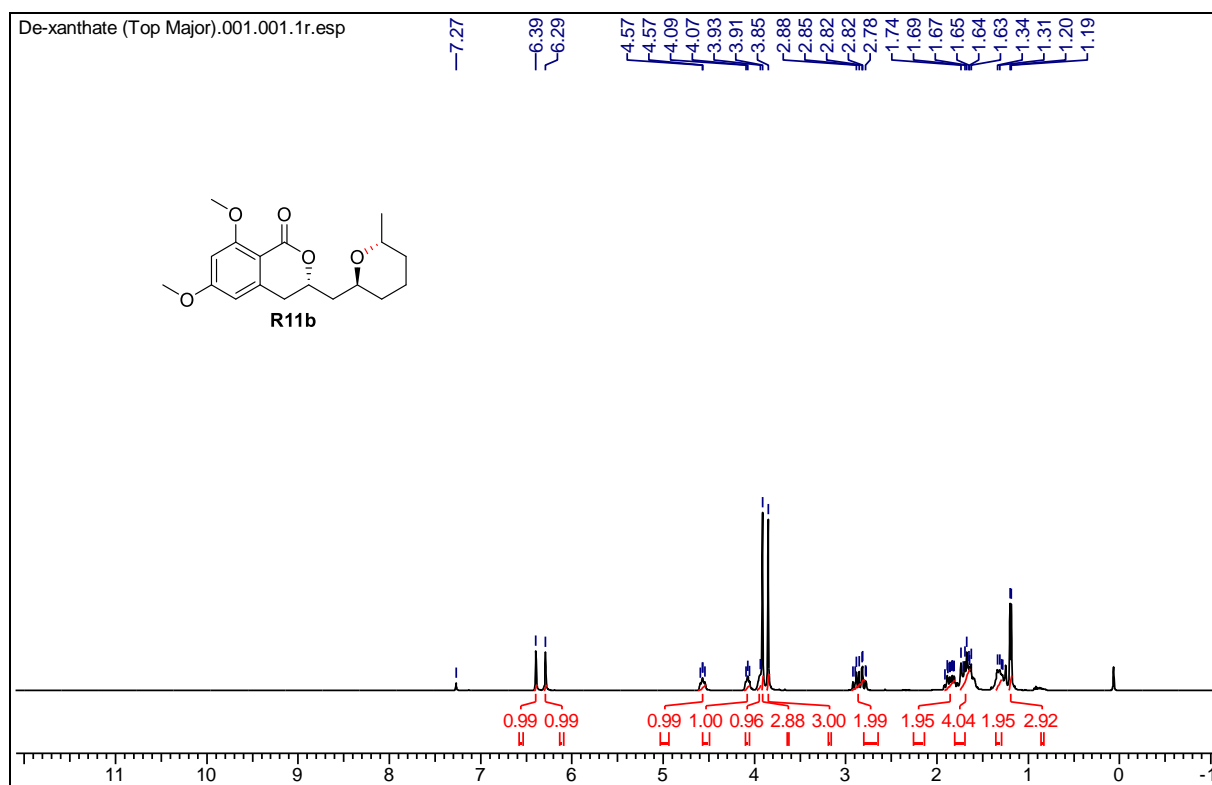
¹H NMR spectra of compound R11a in 400 MHz



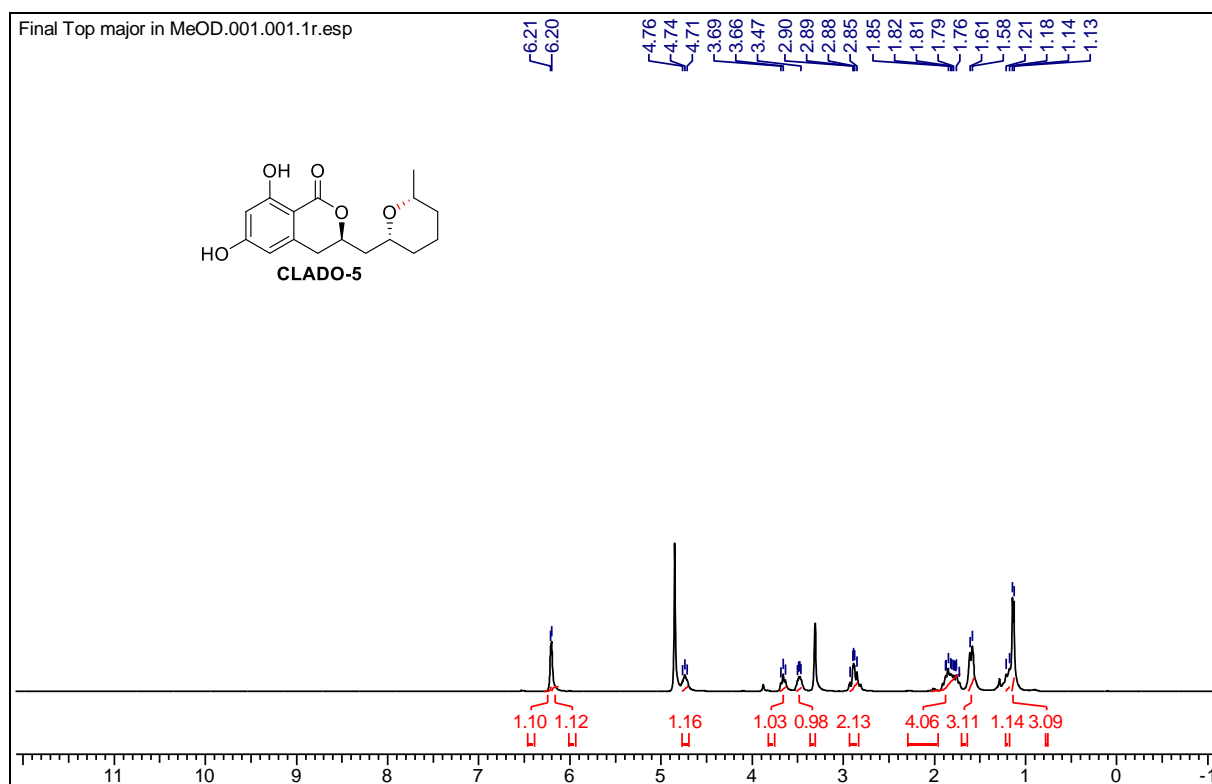
¹H NMR spectra of compound R10b in 400 MHz



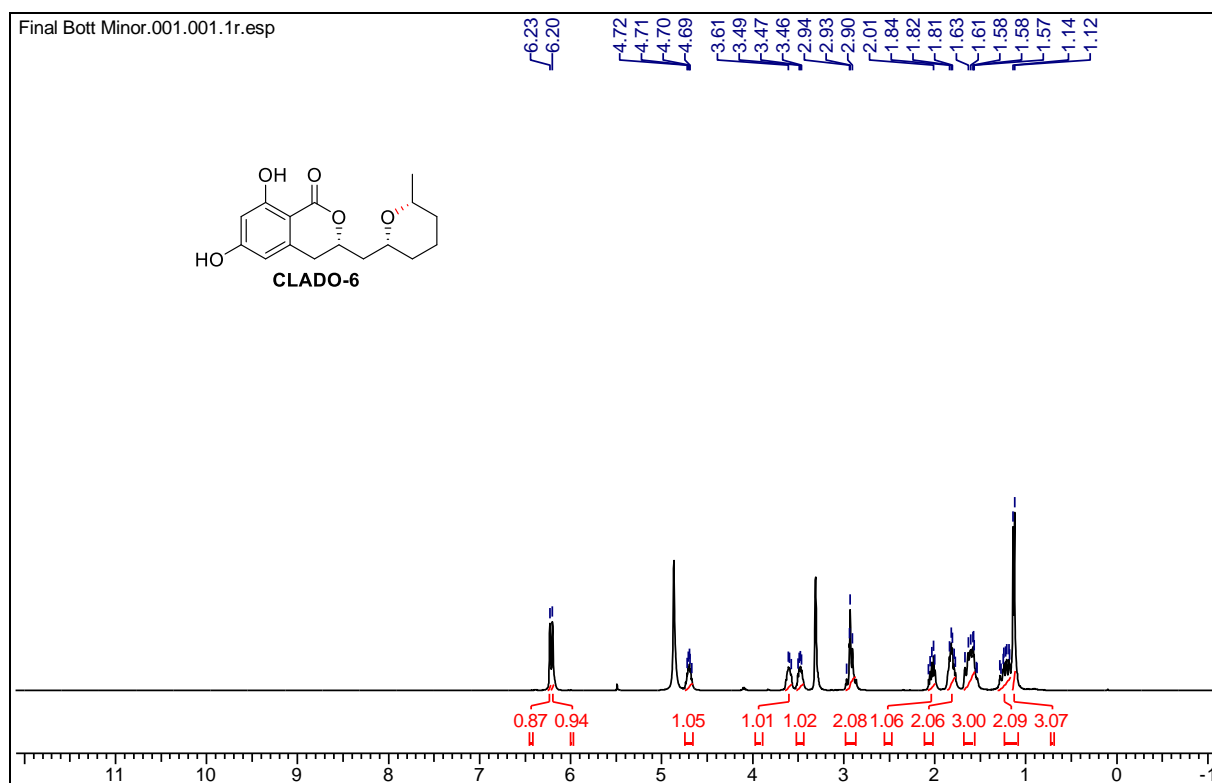
¹H NMR spectra of compound R11b in 400 MHz



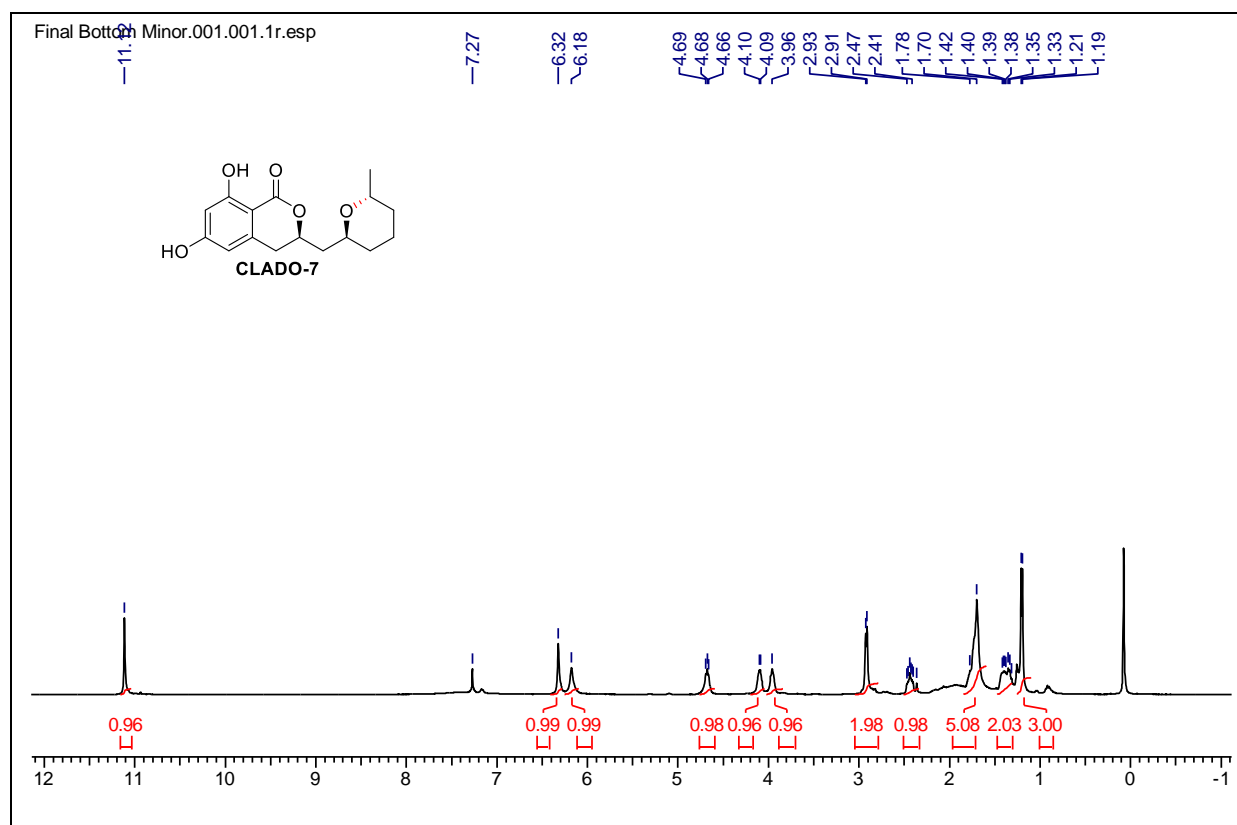
¹H NMR of compound 16



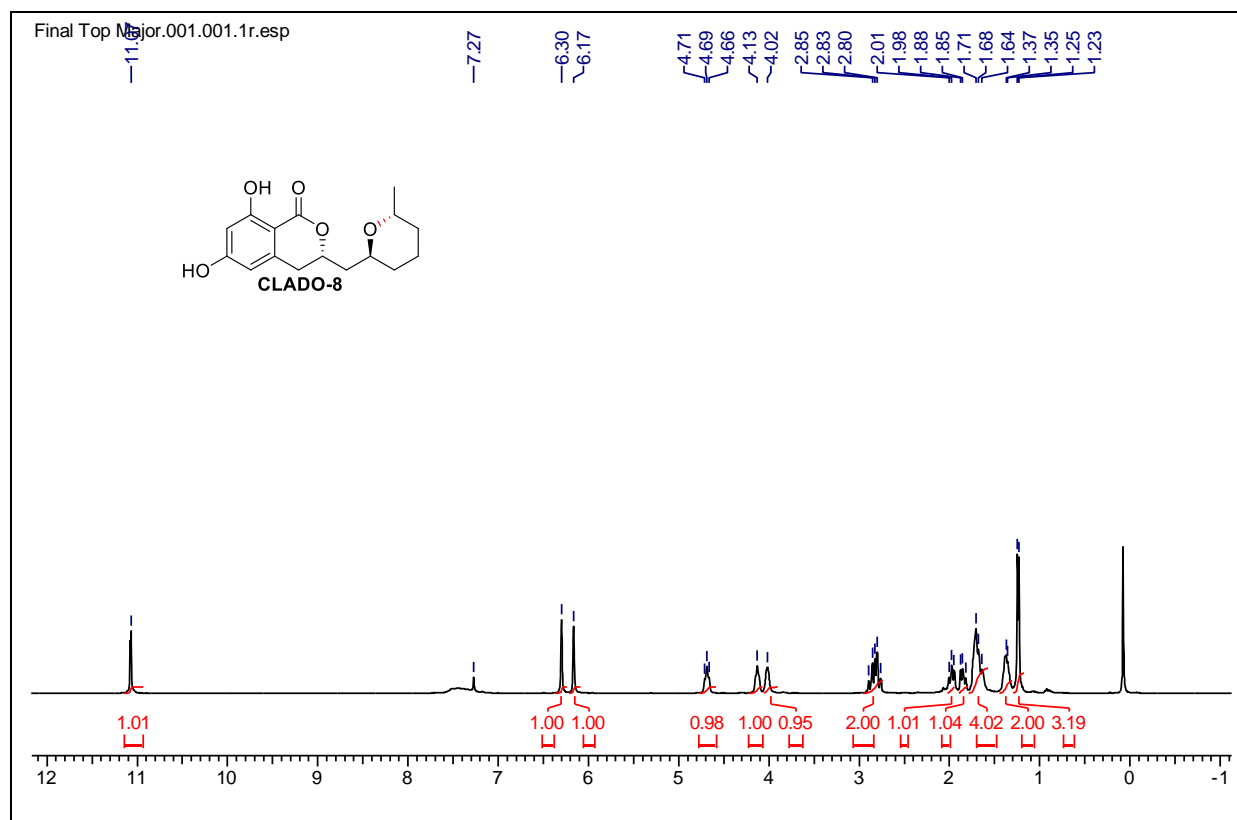
¹H NMR of compound 17



¹H NMR of compound 18



¹H NMR of compound 19



References

- (1) Bruker (2016). *APEX2, SAINT and SADABS*. Bruker AXS Inc., Madison, Wisconsin, USA.
- (2) Sheldrick, G. M. *Acta Crystallogr.*, **2007**, A64, 112-122.
- (3) Barnes, C. L. ORTEP -3 for Windows. *J. Appl. Crystallogr.* **30**, 568–568 (1997).
- (4) Khan, S.; Sharma, A.; Belrhali, H.; Yogavel, M.; Sharma, A. *J. Struct. Funct. Genomics*, **2014**, *15*, 63-71.
- (5) Sharma, A.; Sharma, M.; Yogavel, M.; Sharma, A. *PLoS Negl. Trop. Dis.* **2016**, *10*, 1-19.
- (6) Cestari, I.; Stuart, K. A. *J. Biomol. Screen.* **2013**, *18*, 490-497.
- (7) Trager, W.; Jensen, J. B. *J. Parasitol.* **2005**, *91*, 484-486.
- (8) Tonkin, C. J.; Van Dooren, G. G.; Spurck, T. P.; Struck, N. S.; Good, R. T.; Handman, E.; Cowman, A. F.; McFadden, G. I. *Mol. Biochem. Parasitol.* **2004**, *137*, 13-21.
- (9) Smilkstein, M.; Sriwilaijaroen, N.; Kelly, J. X.; Wilairat, P.; Riscoe, M. *Antimicrob. Agents Chemother.* **2004**, *48*, 1803-1806.
- (10) Kabsch, W. *Acta Cryst. D66*, **2010**, 125-132.
- (11) Waterman, D.G.; Winter, G.; Gildea, R.J.; Parkhurst, J. M.; Brewster, A. S.; Sauter, N. K.; Evans, G. *Acta Crystallogr D Struct Biol.* **2016**, *72*, 558-575.
- (12) Murshudov, G. N.; Skubak, P.; Lebedev, A. A.; Pannu, N. S.; Steiner, R. A. *Acta Crystallogr. D Biol. Crystallogr.* **2011**, *67*, 355-367.
- (13) Adams, P. D.; Afonine, P. V.; Bunkoczi, G.; Chen, V. B.; Davis, I. W. *Acta Crystallogr. D Biol. Crystallogr.* **2010**, *66*, 213-221.
- (14) Emsley, P.; Lohkamp, B.; Scott, W. G.; Cowtan, K. *Acta Crystallogr. D Biol. Crystallogr.* **2010**, *66*, 486-501.
- (15) Winn, M. D.; Ballard, C. C.; Cowtan, K. D.; Dodson, E. J.; Emsley, P. *Acta Crystallogr. D Biol. Crystallogr.* **2011**, *67*, 235-242.
- (16) Chen, V. B.; Arendall, W. B.; Headd, J. J.; Keedy, D. A.; Immormino, R. M. *Acta Crystallogr. D Biol. Crystallogr.* **2010**, *66*, 12-21.
- (17) Pettersen, E. F.; Goddard, T. D.; Huang, C. C.; Couch, G. S.; Greenblatt, D. M. *J. Comput. Chem.* **2004**, *25*, 1605-1612.